Economic Geology 100th Anniversary Volume
pp. 1001–1033

Gold Metallogeny of the Superior and Yilgarn Cratons

François Robert,†
Barrick Gold Corporation, Suite 3700, 161 Bay Street, P.O. Box 212, Toronto, Canada M5J 2S1

K. Howard Poulsen,
34 Wallford Way, Nepean, Ontario, Canada K2E 6B6

Kevin F. Cassidy,
Geoscience Australia, GPO Box 378, Canberra, ACT, 2601, Australia

and C. Jay Hodgson
Barrick Gold Corporation, Suite 3700, 161 Bay Street, P.O. Box 212, Toronto, Canada M5J 2S1

Abstract

The gold-rich Superior, Canada, and Yilgarn, Australia, cratons have similar geologic histories dating back to the Mesoarchean and showing strong parallels in the Neoarchean. Orogenesis in each craton is marked by a shift from dominant volcanism to dominant clastic sedimentation above unconformities, followed by granitic plutonism, progressive deformation, and dynamothermal metamorphism. The terminal stages of orogenesis correspond to the intervals of 2660 to 2650 Ma in the Superior craton and 2660 to 2630 Ma in the Yilgarn craton. The Yilgarn and Superior cratons contain an estimated 9,200 and 8,500 t Au, respectively. Most of the significant gold deposits (>100 t Au) are concentrated in a few narrow, highly endowed gold belts along which the deposits cluster into camps, commonly spaced every 30 to 50 km. Gold deposits of both cratons show similar tonnages and grades, and their size distributions define a Pareto, rather than log-normal distribution. Large deposits are rare but account for most of the gold endowment of each craton.

Three recurring host-rock associations account for a majority of large deposits: iron-rich mafic igneous rocks, iron-rich sedimentary rocks, and felsic to intermediate porphyry stocks and dikes. Most deposits, particularly large ones, occur in greenschist-grade rocks and are associated with shear zones, faults, or folds. Gold mineralization styles include quartz-carbonate veins, sulfidic replacements in banded iron formation (BIF), crustiform carbonate-quartz veins and associated sulfidic replacement lodes, disseminated-stockwork zones, sulfide-rich veins and veinlet zones, and massive sulfide lenses. Wall-rock alteration assemblages vary with mineralization style and metamorphic grade. Most deposits consist of a single style of mineralization, but many of the large ones combine two or more of these, and some large deposits are unique in their metal associations. The diversity of styles of mineralization, wall-rock alteration assemblages, and overprinting relationships require more than one episode of gold mineralization and more than one ore-forming process. Geologic parageneses, coupled with isotopic age constraints, show that, although the Archean histories of both cratons span >300 m.y., the majority of gold deposits formed during the final 30 to 50 m.y. of that time span, corresponding to the orogenic phase. The majority of gold deposits can thus be regarded as orogenic in timing, but with the available constraints clearly pointing to the existence of more than one mineralizing event and involving different mineralization types and processes.

The best-endowed gold camps (Timmins and Red Lake in the Superior craton; Kalgoorlie, Granny-Wallaby, and Sunrise Dam in the Yilgarn craton) commonly possess an anticlinorial structure, komatiitic and basaltic rocks in the core giving way to stratigraphically higher volcanic and clastic sedimentary rock units. Such camps are further marked by coarse clastic rocks deposited above the metavolcanic rock sequences, by concentrations of shallow-level porphyritic intrusions, by extensive carbonate alteration, by multiple styles and ages of gold mineralization and, in most, by through-going regional faults. However, these characteristics are also shared by a number of less-endowed gold camps. The best-endowed gold belts are distinguished by substantial volumes of komatiite, by a high degree of preservation of supracrustal rocks, by structural highs that juxtapose the lower and uppermost parts of the stratigraphic column, by multiple styles and ages of gold mineralization, and by world-class deposits of other metals. The gold belts commonly are aligned along crustal-scale faults that represent long-lived structures, which acted as crustal-scale magma and fluid conduits and also influenced coarse clastic sedimentation. Abundant komatiites may reflect the first tangible connection to the deep crust and mantle, but the nature of the subvolcanic crust, ensimatic in the Timmins-Val d'Or, Superior craton, and ensialic in the Wiluna-Norseman belts, Yilgarn cration, seems unimportant in determining gold prospectivity.

Significant uncertainty remains concerning the timing of formation of the deposits, the models that best explain their characteristics, and the fundamental causes of the high concentration of gold in a few areas. Various models have been proposed, invoking volcanic, magmatic, and orogenic (metamorphism and/or deformation) processes. The synorogenic model best accounts for the Au-only quartz-carbonate veins and temporally related

† Corresponding author: e-mail, frobert@barrick.com

mineralization styles. However, synvolcanic and magmatic hydrothermal models are also required to explain the presence of Au base metal deposits and those deposits overprinted by significant deformation and metamorphism. The specific histories of the gold belts and the known constraints on timing of deposits suggest that all of these processes have contributed to the gold endowment, although it is difficult to separate orogenic from magmatic processes because they closely overlap in time and space.

Despite the presence of synorogenic quartz-carbonate veins throughout the greenstone belts of both cratons, large deposits of this style are mainly restricted to the gold belts, where they also coexist with large deposits of other styles of gold mineralization. The presence of multiple ages and styles of gold mineralization in the best-endowed gold belts indicate a unique locus of successive formation of gold deposits from various processes operating at different stages of the orogenic phase of the evolution of these belts. This would explain the common overprinting of the early deposit types, potentially of synvolcanic or synplutonic origin, by synorogenic ones. The concentration of multiple types and ages of significant gold deposits in well-defined gold belts is not a unique feature of the Superior and Yilgarn cratons but is shared by Tertiary gold belts of Nevada, such as the Walker Lane, the Battle Mountain-Eureka trend, and the Carlin trend. This must be a reflection of fundamental crustal structure, and perhaps composition of subcrustal mantle, as much as local ore-forming hydrothermal processes.

Introduction

The Yilgarn and Superior cratons in Western Australia and central to east Canada (App. Fig. A1), with >9,200 tons (t) and >8,500 t Au, respectively, account for approximately 75 percent of the gold in Archean greenstone belts (Goldfarb et al., 2001). By virtue of their large area and gold endowment, these two cratons and their gold deposits have influenced the development of concepts related to Archean tectonics and economic geology over the past 100 years.

Influenced by the empirical observation that gold deposits are rarely found in regions without exposed igneous bodies, researchers in the first half of the twentieth century (e.g., Lindgren, 1933; Emmons, 1937) drew heavily on field examples from both cratons to support the idea that Archean gold deposits are mainly of magmatic hydrothermal origin. Observed variations among deposits were mainly attributed to differences in depth of formation, which led to the formulation of several empirical criteria to explain where gold deposits could be found (Emmons, 1937). These were the first documented attempts to define the metallogeny of Archean gold deposits and geologic criteria for target selection, as distinct from genetic models and ore genesis.

The second half of the twentieth century saw a shift toward alternative hypotheses concerning deposit genesis and metallogeny, particularly with the high economic interest in gold during the past 25 years. Modern data led to proposals that a large number of gold deposits are orogenic, i.e., related to metamorphic processes (Groves and Phillips, 1987) or intrusion-related (Spooner, 1993; Goldfarb et al., 2005). Other deposits have also been argued to be the products of submarine hydrothermal systems (Hutchinson, 1993) or the deformed and metamorphosed equivalents of shallow epithermal and porphyry deposits (Penczak and Mason, 1997). In each case, a different timing and setting of gold deposition are implicit, resulting in different interpretations of the relative importance of the various empirical attributes of the deposits. Despite intensive gold-related research over the past 25 years, a number of these relationships are still debated (see Groves et al., 2003).

The objectives of this regional metallogeny paper are to discuss the time-space-size distribution of gold deposits in relationship to key geologic features of their host environments, and examine the key regional and local controls on deposit locations in these two cratons. Implications for the genesis of the deposits and their exploration are also highlighted. The approach is to first review the spatial and size distribution of gold deposits in the cratons, and then examine key recurring geologic features at the deposit, camp, and belt scales.

Overview of the Superior and Yilgarn Cratons

The Superior craton (Fig. 1) occupies an area of approximately 2 Mkm^2, about twice the size of the Yilgarn craton (Fig. 2). Both cratonic masses have similar geologic characteristics and are likely the remnant nuclei of one or more extensive Mesoarchean and Neoarchean cratons, now surrounded and truncated by Proterozoic orogens (Card, 1990; Myers, 1995). The internal parts of the cratons have remained largely stable since the end of the Archean. The cratons have historically been subdivided into smaller tectonic entities (Figs. 1, 2) but, in recent years, smaller subdivisions have been made to account for variations in age, rock type, metamorphism, and geophysical characteristics. Because the details of the successive levels of subdivision are complex and continue to evolve, a simplified nomenclature is used in this paper. The term "craton" applies to both Superior and Yilgarn, the former divided into "subprovinces" (Card, 1990) and the latter into "provinces" (Myers, 1995), in accord with common usage. Further subdivision into "belts," in both a tectonic and metallogenic sense, is equivalent to the domains or terranes of other authors. Specific lithostratigraphic units within belts and camps are termed "groups" but may be equivalent to the assemblages of some authors.

The Superior craton (Fig. 1) shows a well-defined arrangement of east-west volcano-plutonic subprovinces (e.g., Abitibi, Wabigoon, Uchi), which are separated by subprovinces dominated by metasedimentary and gneissic rocks (e.g., Pontiac, Quetico, English River). This east-west pattern is interrupted by the north-northeast–trending Kapuskasing structure, a Paleoproterozoic east-verging thrust zone that exposes deeply eroded Archean crust in its hanging wall. The Yilgarn craton displays a broadly north-south arrangement of volcano-plutonic provinces (e.g., Eastern Goldfields, Southern Cross, Murchison) and gneissic belts (e.g., Narryer and South West Gneiss) but through-going belts of metasedimentary rocks are lacking (Fig. 2).

Diverse tectonic interpretations have been proposed to explain the development of these Archean cratons. Early models relied heavily on geosynclinal theory and related mountain-building processes (Hutchinson et al., 1971; Groves and Batt,

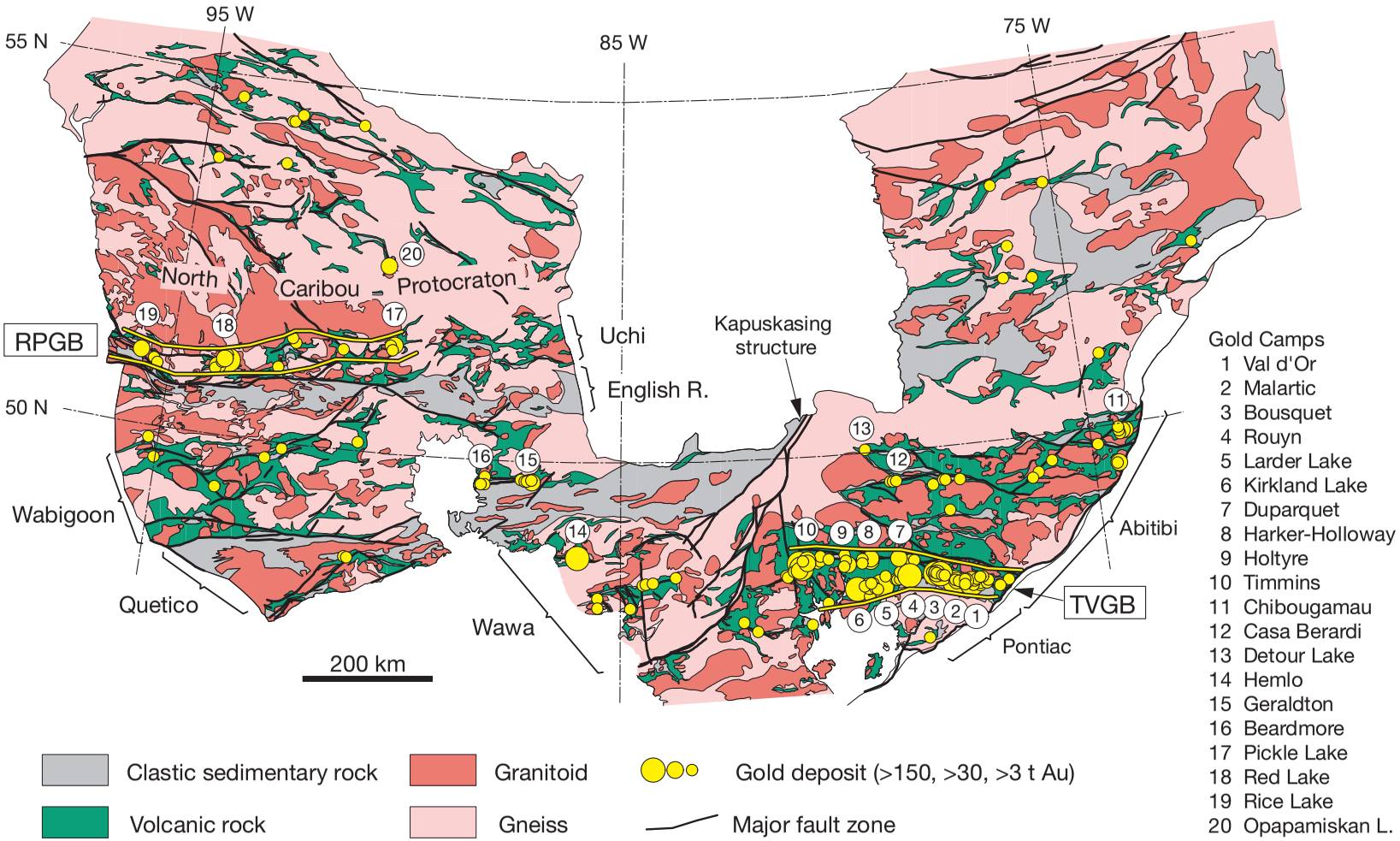

FIG. 1. Simplified geologic map of the Superior craton, showing the main subprovinces and significant gold deposits and camps. Modified from Card (1990) and Card and Poulsen (1998). RPGB = Rice Lake-Pickle Lake Gold belt, TVGB = Timmins-Val d'Or gold belt.

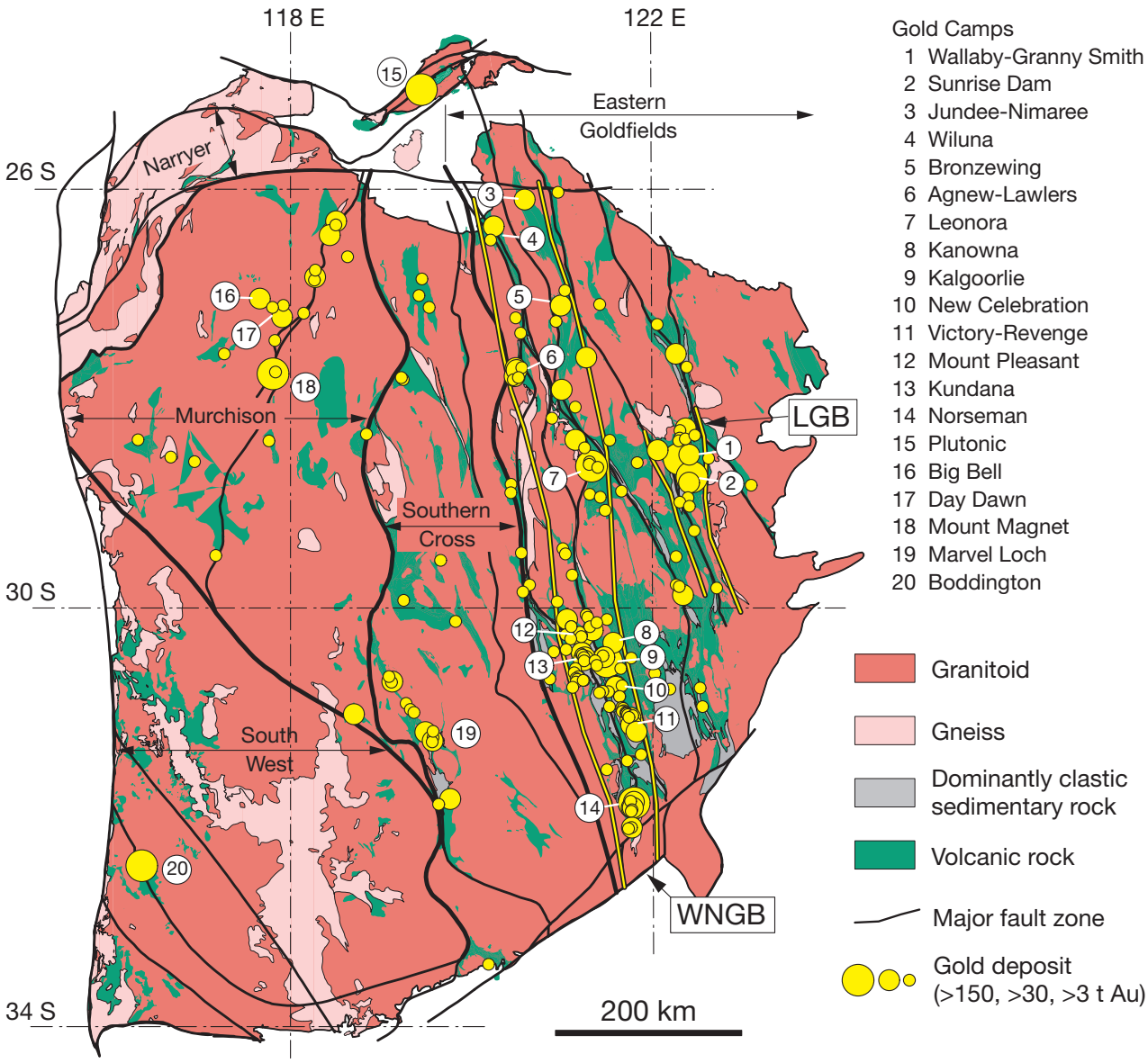

FIG. 2. Simplified geologic map of the Yilgarn craton, showing the main subprovince boundaries and significant gold deposits and camps. Modified from Myers (1995).

1984), dominated by autochthonous greenstone development on sialic crust and followed by closing of volcanic-sedimentary basins during compressional orogeny. Various plate tectonic models involving subduction and accretion of diverse crustal fragments have generally supplanted the older models and typically highlight the importance of accretionary tectonics to the growth of the cratons (Card, 1990; Myers, 1995). Some recent models also stress the importance of both mantle plumes and long-lived convergent margin tectonics (Barley et al., 1998; Percival, 2003).

The chronology of Archean events is similar for both cratons, with major addition of crust at ~3020 to 2920 and 2760 to 2660 Ma (Fig. 3) to now scattered remnants of pre-3100 Ma high-grade gneisses and supracrustal rocks (Myers, 1995; Percival 2003). In the Yilgarn craton, most Mesoarchean rocks are preserved in the Murchison and Southern Cross provinces, where they include 3020 to 2810 Ma ultramafic, mafic, and felsic volcanic and sedimentary rocks (Pidgeon and Hallberg, 2000; Cassidy and Champion, 2004), with minor occurrences in the Eastern Goldfields province. The Murchison and Southern Cross provinces were likely a single entity by at least 2810 Ma (Cassidy and Champion, 2004). The Superior craton includes areas underlain by >2800 Ma continental crust separated by belts of younger oceanic material (Percival, 2003). The largest area is represented by the ~3000 Ma North Caribou protocraton (Stott, 1997; Fig. 1). Along its southern margin, volcanic arc rocks of the Uchi subprovince were deposited over a 300-m.y.-long period prior to a ~2710 Ma collision. Rift sequences deposited between about 2850 and 2800 Ma are also partly preserved in the Superior craton (Percival, 2003).

The Yilgarn and Superior cratons have strong parallels in their Neoarchean histories, which account for most rocks in

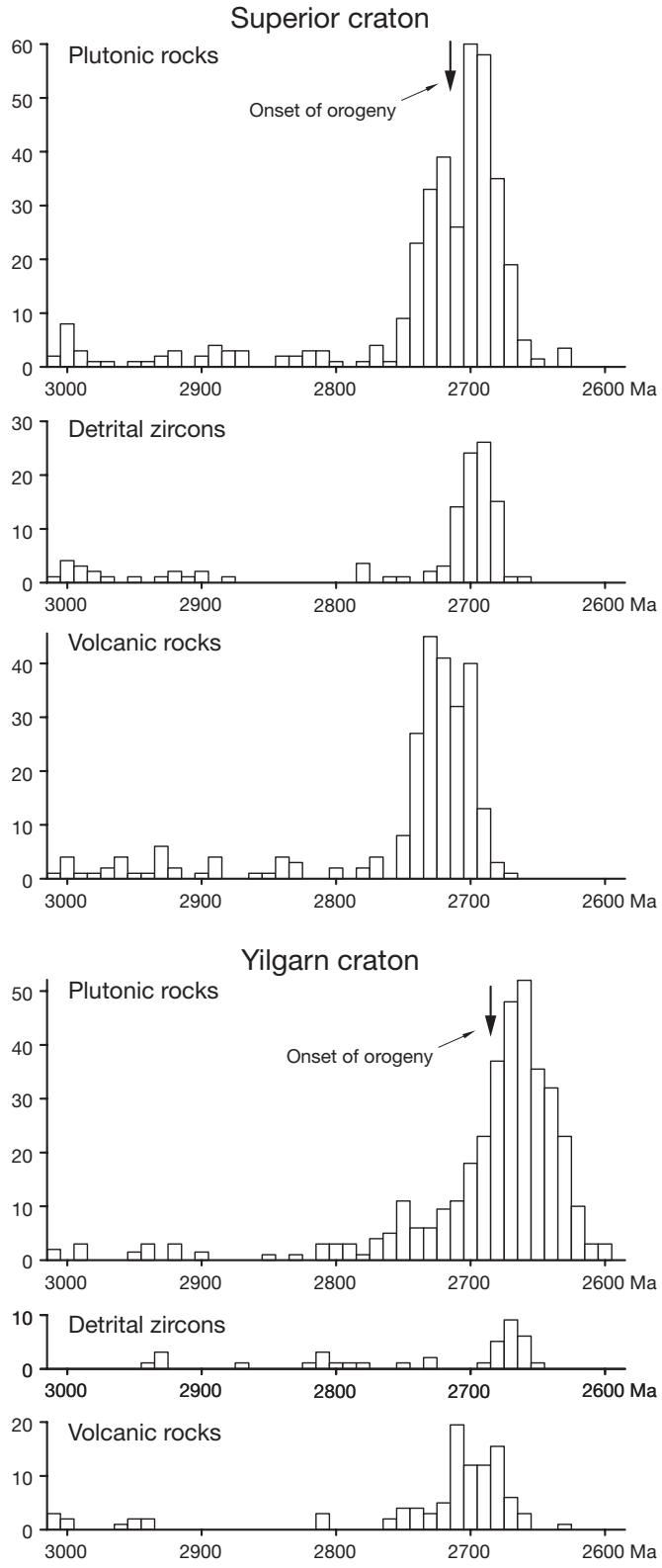

FIG. 3. Histograms showing the distribution of ages of volcanic and plutonic rocks and detrital zircons for the Superior and Yilgarn cratons. Superior data from Corfu and Davis (1992), Corfu and Stott (1993), Card and Poulsen (1998), Skulski and Villeneuve (1999), and Ayer et al. (2002). Yilgarn data from Pidgeon and Hallberg (2000), Myers (1995), Nelson (1997), Krapez et al. (2000), and Cassidy et al. (2002).

these cratons (Fig. 3). A period of more than 50 m.y. of nearly continuous volcanism and coeval plutonism began in the Yilgarn craton, with felsic volcanism in the southern Murchison and Southern Cross provinces at ~2760 to 2730 Ma (Pidgeon and Hallberg, 2000), followed by the emplacement of voluminous volcanic and plutonic rocks between 2720 and 2660 Ma in the Eastern Goldfields province. In the Superior craton, the comparable volcanic interval began at approximately 2750 Ma, with widespread volcanic arc formation that continued through 2715 Ma in the northern, 2705 Ma in the central, and 2695 Ma in the southern parts of the craton. The mafic volcanic sequences in both cratons are dominated by tholeiitic and komatiitic rocks and commonly are overlain by mainly calc-alkaline felsic to intermediate volcanic rocks in many greenstone belts.

In both cratons, the decline in volcanism corresponds to an increase in clastic sedimentation (Fig. 3). In the Superior craton, these clastic sedimentary rocks are commonly subdivided into wacke-mudstone groups of dominantly turbiditic origin (e.g., Porcupine and Cadillac Groups) and conglomerate and arenite groups, locally with turbiditic rocks, of shallow marine, fluvial, and alluvial origins (e.g., Timiskaming Group, San Antonio Formation; Card and Poulsen, 1998). Some of the turbiditic rocks form extensive belts of graywacke-mudstone flysch in the Pontiac, Quetico, and English River subprovinces, but turbidites, conglomerates, and arenites also occupy basin remnants within the volcano-plutonic subprovinces. Comparable suites of sedimentary rocks in the Yilgarn craton are represented by the Black Flag Group and by the late-stage basins (Kurrawang, Jones Creek,Yilgangi) of the Eastern Goldfields province (Krapez et al., 2000). The onset of sedimentation appears to lag that in the Superior craton by about 20 m.y. (Fig. 3). At many localities in both cratons, such sequences are deposited above disconformities, unconformities, and nonconformities, suggestive of synorogenic sedimentation (Mueller and Donaldson, 1992; Krapez et al., 2000).

Plutonism accompanied and outlasted clastic sedimentation in both cratons (Fig. 3). Rocks of the Black Flag Group in the Eastern Goldfields province have a tonalite-trondhjemite-granodiorite igneous rock provenance but are cut by ~2655 Ma postsedimentation granitoids (Nelson, 1997). Later stage, Yilgarn-wide low Ca granites were emplaced at 2650 to 2630 Ma (Cassidy et al., 2002; Champion and Cassidy, 2002). This equates to the so-called 2670 to 2650 Ma "late granite bloom" of Percival (2003) in the Superior craton that, like sedimentation, appears to be about 20 m.y. older than widespread Yilgarn magmatism. Myers (1995) also noted the dominance of granitic intrusions (sensu stricto) in the Yilgarn, compared to the importance of tonalite and granodiorite in the Superior craton (Card, 1990).

The intense folding, metamorphism, and plutonism that mark the end stages of Neoarchean history are commonly attributed to orogeny (e.g., Swager, 1997; Card and Poulsen, 1998; Weinberg et al., 2003). There is considerable evidence to suggest diachroneity of orogeny, especially if the onset of orogeny is defined as the onset of clastic sedimentation above angular unconformities (Corfu and Davis, 1992; Krapez et al., 2000; Daigneault et al., 2002; Blewett et al., 2004). In the case of the Superior craton, successive collisional events range in

age from 2720 to 2710 Ma in the northern part of the craton to about 2680 Ma in the southern part. The terminal stage of orogeny corresponds to the interval 2660 to 2650 Ma and to 2660 to 2630 Ma in the Superior and Yilgarn cratons, respectively (Fig. 3).

The greenstone belts of the Superior and Yilgarn cratons have generally experienced similar deformation histories, involving a limited number of folding, shearing, and faulting events, typically ascribed to distinct increments of deformation (D_1, D_2, etc). Despite the uncertainties of correlation of deformational events from place to place, a common sequence of events is evident, and such a deformational nomenclature is used throught this paper to convey comparative information about the deformational history. Early, commonly elusive, D_1 deformation predates, or is synchronous with, sedimentation and tends to take place without significant development of penetrative fabrics. Regional folds and shear zones, as well as regional dynamothermal metamorphic foliation and lineation, characterize D_2 deformation and overprint metavolcanic and metasedimentary rocks of all ages. The D_2 event commonly accounts for the greatest penetrative strain. Late-stage open folds, crenulation cleavages, and other shear zones and faults are commonly assigned to D_3. There is also increasing evidence for extensional events between some of these contractional deformation events (Swager, 1997; Ayer et al., 2002).

Despite the many similarities between the two cratons, there are notable differences. The clear pattern of alternating metasedimentary and granite-greenstone belts, so prominent in the Superior craton, is absent in the Yilgarn craton, reflecting the absence of extensive metasedimentary belts in the latter. The wacke-mudstone sequences that dominate in subprovinces such as the Pontiac, Quetico, and English River (Fig. 1) are not in evidence in the Yilgarn craton (Fig. 2). Areas of medium- to high-temperature, low-pressure metamorphism, typical of the metasedimentary subprovinces of the Superior craton (Card and Poulsen, 1998), are more restricted in the Yilgarn craton (Myers, 1995). Despite the commonality of major Archean gold deposits, a striking metallogenic difference is that the Yilgarn craton is renowned for its komatiite-associated nickel ores and a paucity of Fe-Cu-Zn volcanogenic massive sulfide (VMS) deposits (Groves and Batt, 1984), whereas the converse is true for the Superior craton (Card and Poulsen, 1998).

Spatial and Size Distribution of Deposits

Hundreds of gold deposits of varying size are distributed throughout the Yilgarn and Superior cratons but, for the purpose of this review, only those containing >3 t Au (production plus reserves[1]) are considered. As shown in Figures 1 and 2, gold deposits and occurrences of the two cratons are almost exclusively restricted to the greenstone belts, among which large deposits are unevenly distributed. Most of the gold in the Superior craton is concentrated in the greenstone belts of the Abitibi (6,000 t Au) and the Uchi (1,000 t Au) subprovinces (Fig. 1), whereas most gold in the Yilgarn craton is concentrated in greenstone belts of the Eastern Goldfields (7,000 t Au) and Murchison (900 t Au) provinces (Fig. 2). The gold endowment of individual greenstone belts appears to partly correlate with the ratio of supracrustal to granitic rocks, which is higher in Abitibi and Eastern goldfields than in Wabigoon and Murchison, respectively (Figs. 1, 2).

Within the productive greenstone belts, the significant deposits commonly cluster into mining camps (Figs. 1, 2), covering on the order of 100 to 1,000 km^2 (Hodgson, 1993). Camps may be defined by a single large deposit among a cluster of small occurrences, as is the case for the Hemlo, Kirkland Lake, Boddington, and Plutonic camps, or by a cluster of several individual deposits, as in the case of the Timmins and Kalgoorlie camps. Gold camps in both cratons commonly define curvilinear belts that are typically 50 to 100 km wide and 200 to 1,000 km long and are aligned along major crustal structures (Figs. 1, 2). The two largest and best-defined gold belts in the Superior craton are the Timmins-Val d'Or (5,600 t Au) and Rice Lake-Pickle Lake (975 t Au). Wiluna-Norseman (5,225 t Au), and Laverton (850 t Au) in the Eastern Goldfields province are the most significant belts of the Yilgarn craton.

Gold deposits display a similar spectrum of sizes and average grades in both cratons (App. Fig. A2), although the grades of the bulk of the Superior craton deposits are slightly higher than those of the Yilgarn craton. The lower mined grades in the Yilgarn craton likely reflect the presence of deep oxidation, which has permitted open-pit mining of lower grade deposits, whereas in the glaciated Superior craton, most of the operations are underground and hence have higher cutoff grades. The size distribution of gold deposits, in terms of both numbers of deposits and cumulative tons (App. Fig. A3), emphasizes the facts that large deposits are rare compared to smaller ones and that they account for most of the gold endowment. In the Superior craton, for example, approximately ten times as many deposits contain 100 than 1,000 t Au, and ten times as many contain 10 than 100 t Au (Fig. A3A), defining a Pareto (hyperbolic), rather than log-normal size distribution (Agterberg, 1995). The 39 largest deposits in the Superior craton (~21% of the total number) and the 42 largest in the Yilgarn craton (also 21% of the total) account for 80 percent of the gold endowment of their respective cratons, showing a good fit to the long-established 80/20 rule.

The cumulative frequency distributions of contained gold in the cratons are similar for deposits containing ≤100 t Au but are markedly different for deposits with >300 t Au (Fig. A3B). The Superior craton contains eight deposits with >300 t Au, compared to only three for the Yilgarn craton, although the Yilgarn does contain the single largest deposit. It is not clear if this difference in the number of large deposits reflects a primary difference in endowment or a difference in exploration maturity. There are also differences in the overall size distribution of >100-t Au camps in the Superior and Yilgarn cratons (App. Fig. A4). The Superior craton hosts nine camps containing >300 t Au compared to only five in the Yilgarn. In contrast, the Yilgarn hosts 15 camps containing 100 to 300 t Au, compared with only two in that category in the Superior craton.

[1] Figures used are based on production and reserves, and include measured and indicated resources where reported separately from inferred resources. Because of different reporting procedures, it was not always possible to separate inferred resources for the Australian deposits, which tends to inflate the total endowment of Yilgarn relative to Superior.

Characteristics of Gold Deposits

Gold deposits of the Superior and Yilgarn cratons display a significant spectrum of mineralization, structural, and geometric characteristics (Figs. 4, App. A5; Colvine, 1989; Hodgson, 1993; Groves et al., 2003). They are also commonly grouped into Au-only and Au-base metal categories, reflecting variations in ore composition as well (e.g., Groves et al., 2003). A number of styles of mineralization, typically forming individual orebodies in gold deposits, can be defined from a descriptive point of view (Table 1). Many deposits in both cratons consist of a single style of mineralization but many others, especially the larger ones, consist of two or more styles.These different mineralization styles also combine with specific lithologic and structural settings to form a number of recurring deposit-scale associations.

Recurring lithologic and structural settings

Lithologically, gold deposits occur in all rock types in greenstone belts of the Superior and Yilgarn cratons, but three rocks types host the majority of large deposits: iron-rich mafic igneous rocks, such as tholeiitic basalt and differentiated dolerite sills; iron-rich clastic metasedimentary rocks and banded iron formation (BIF); and dioritic to felsic porphyritic stocks and dikes (Table 1). Conversely, few deposits are hosted in felsic volcanic rocks, in large granitoids bodies, or in clastic metasedimentary rocks, except where associated with intermediate to felsic intrusions. Iron-rich rocks, especially those with a high Fe/(Fe + Mg) content, are chemically favorable hosts (Phillips et al., 1984; Böhkle, 1989), whereas intermediate to felsic porphyry intrusions are favorable structural hosts because of their brittle response to regional deformation that leads to enhanced fracturing and veining (cf. Cassidy et al., 1998). Some lithologic units, such as iron-rich sedimentary rocks and granophyric layers within differentiated dolerite sills, are particularly favorable hosts because of their combined iron-rich and competent, brittle nature. Specific lithologic associations also dominate in some greenstone belts or camps. For example, gold deposits of the Wiluna-Norseman belt are commonly associated with differentiated dolerite sills (Groves et al., 1995), whereas those of the Timmins-Val d'Or belt are commonly associated with shallow-level porphyry intrusions (Hodgson, 1993).

Although gold deposits occur in rocks metamorphosed from lower greenschist to upper amphibolite grades, the majority occurs in greenschist-grade rocks (Goldfarb et al., 2005). Only a few large deposits occur at the greenschist to amphibolite transition (Campbell-Red Lake: Andrews et al., 1986; Norseman: McCuaig et al., 1993) or in amphibolite-grade rocks (Hemlo, Musselwhite, Big Bell, and Plutonic), and some of these have clearly been metamorphosed (Big Bell: Phillips, 1985; Hemlo: Lin, 2001). Very few deposits occur in subgreenschist-facies rocks (Wiluna: Hagemann et al., 1992), and no deposits of significance occur in granulite-grade rocks.

Structurally, gold deposits in both cratons are universally associated with shear zones, faults, or folds (Table 1). Such an association reflects a strong structural control on the localization and development of mineralization and also the tendency for less-competent altered rocks to localize subsequent deformation (Robert and Poulsen, 2001). Mineralized shear zones are typically high-order structures adjacent to the more regional structures along which the gold camps and large deposits are located (Goldfarb et al., 2005). The character and alteration assemblages of mineralized shear zones and folds generally reflect the ambient metamorphic grade (Colvine, 1989; McCuaig and Kerrich, 1998). Thus, ore-hosting structures range from brittle shear zones and open folds in areas of lower greenschist grade, to brittle-ductile shear zones in mid to upper greenschist-grade rocks, and to ductile shear zones and tight to isoclinal folds at amphibolite or higher grades.

Three particularly favorable combinations of lithologic and structural settings can be defined (Groves et al., 1990). The first consists of shear zones and faults developed along contacts between units of contrasting competencies, such as mafic-ultramafic volcanic rock contacts (Kerr-Addison, Jubilee), or the margins of granitic intrusions (Tarmoola, Granny Smith), or along thin and incompetent lithologic units. Competent rock units enclosed in less competent ones represent a second combination that favors fracturing and veining, such as felsic dikes and stocks in clastic sedimentary rocks (Malartic, Kanowna Belle, Wallaby) or granophyric layers in differentiated dolerite sills (Mount Charlotte, Golden Mile, Victory-Defiance, Darlot-Centenary, San Antonio). Finally, fold hinges and anticlines are a particularly favorable setting for deposits hosted in layered rocks units such as BIF (Musselwhite) and clastic sedimentary rocks.

Styles of gold mineralization

The characteristics of the different styles of mineralization, their most common associated alteration assemblages, and their dominant metal associations are summarized in Table 1. These different mineralization styles also combine with specific lithologic and structural settings to produce a number of recurring deposit-scale associations that can guide exploration but that convey no classification (i.e., deposit style) or genetic implications. Many deposits consist of a single mineralization style but others, especially large ones, combine two or more styles.

Quartz-carbonate veins: Quartz-carbonate veins are the most common mineralization style in both cratons and typically constitute the orebodies in classical orogenic gold deposits (Hodgson, 1993; Hagemann and Cassidy, 2000). These veins commonly form complex, vertically extensive networks (Fig. A5A) that combine various proportions of laminated fault-fill veins in brittle-ductile shear zones (Fig. 4A) and stacked to multidirectional arrays of extensional veins in competent host rocks (Fig. 4B; Groves et al., 1995; Robert and Poulsen, 2001). The quartz-carbonate vein networks are commonly centered on clusters of intermediate to felsic stocks and dikes (Sigma-Lamaque, Kirkland Lake, Dome, Hollinger-McIntyre) or confined to differentiated dolerite sills (Mount Charlotte, Victory-St-Ives, San Antonio). The first association is well illustrated by the Sigma-Lamaque deposit, where a vertically extensive system of quartz-tourmaline-carbonate veins overprints a swarm of steeply dipping feldspar porphyry dikes, scattered and steeply plunging diorite-granodiorite pipes, and a synvolcanic diorite porphyry intrusion (Fig. A5A; Robert and Poulsen, 1997). The second association is illustrated by the Mount Charlotte deposit (Fig.

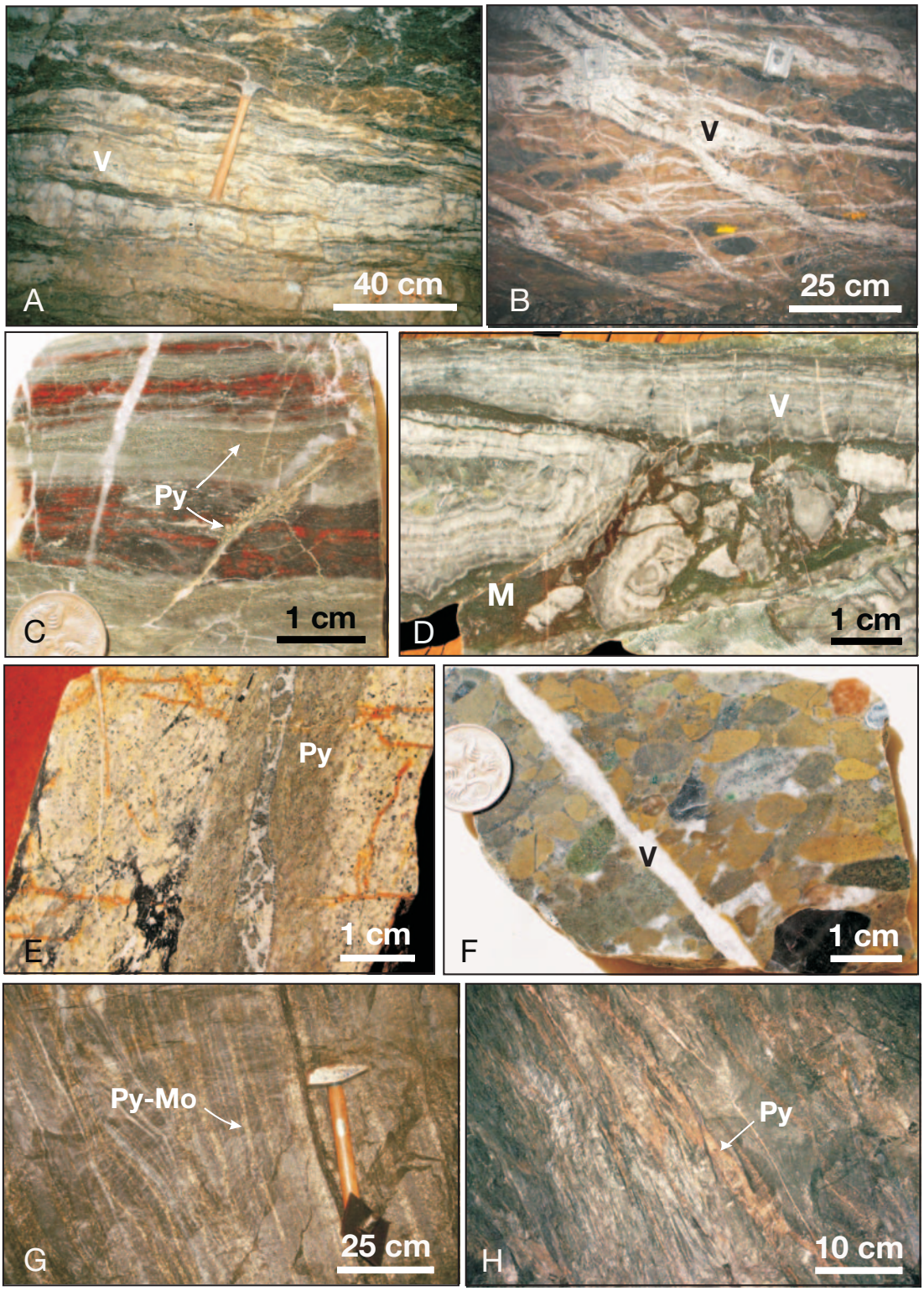

FIG. 4. Photographs of representative styles of gold mineralization in the Superior and Yilgarn cratons. A. Section view of shear zone-hosted laminated fault-fill vein (V), from the Pamour deposit, Superior. B. Section view of an array of extensional veins (V) and alteration selvages (buff color), from the Centenary deposit, Yilgarn. C. Pyrite replacement (Py) of Fe-rich layer from BIF from the Sunrise Dam deposit, Yilgarn. D. Colloform-crustiform banded vein (V) and breccia with fine-grained, high-grade siliceous matrix (M) from the Jundee deposit, Yilgarn. E. Pyritic replacement lode (Py) with thin central breccia from Golden Mile deposit, Yilgarn. F. Fine disseminated pyrite mineralization (small shiny dots) and carbonate-quartz veinlet (V) overprinting albite-sericite-carbonate–altered conglomerate from the Wallaby deposit, Yilgarn. G. Section view of foliated, disseminated pyrite and molybdenite layers (Py-Mo) in high-grade ore from the Hemlo deposit, Superior. H. Section view of transposed sulfide-rich veins (V) in quartz-sericite schist from the Doyon deposit, Superior.

TABLE 1. Characteristics of the Main Styles of Mineralization in Superior and Yilgarn Gold Deposits.

Style of mineralization	Characteristics	Associated alteration assemblages	Metal association	Selected examples where mineralization type is dominant or important (>5 Moz examples in bold character)
Quartz-carbonate veins	Quartz veins with <25% carbonate, <10% sulfide, ±albite, tourmaline, scheelite Vein types include laminated fault-fill and extensional veins Sulfides are mainly pyrite, with arsenopyrite and pyrrhotite	Carbonate-sericite-(albite)-pyrite (arsenopyrite), at greenschist grade Biotite-actinolite-pyrite ± carbonate, at lower amphibolite grade Biotite-calc-silicate-pyrrhotite ± pyrite at mid amphibolite grade	Au > Ag As, W ± Te, Mo, B	Superior: **Hollinger-McIntyre, Kirkland Lake, Sigma-Lamaque**, San Antonio Yilgarn: **Mount Charlotte, Victory-Defiance, Norseman**, Centenary, Bayleys, Westonia
Sulfidic replacements in BIF	Strata-bound replacements of Fe-rich layers by mainly pyrite, arsenopyrite, or pyrrhotite Associated with quartz veins or zones of veinlets or silica flooding	Pyrite (arsenopyrite)-sericite-chlorite-carbonate at greenschist grade Pyrrhotite (loellingite) grunerite-garnet at amphibolite grade	Au > Ag As ± Cu	Superior: Musselwhite, Cockshutt-McLeod, Pickle Crow Yilgarn: Mount Magnet, Mount Morgans, **Sunrise Dam** (in part), Nevoria
Sulfidic replacements and crustiform veins	Crustiform-colloform carbonate-quartz veins and breccias, with various proportions of sulfidic replacements of wal rocks or vein carbonates Sulfides are pyrite or arsenopyrite; stibnite and tellurides abundant in some deposits	Sericite-carbonate-(albite)-pyrite at greenschist grade Biotite-carbonate-silica ± alumino-silicate at amphibolite grade	Au > Ag, As, Te, ± Sb, Hg, W, Zn	Superior: **Campbell-Red Lake** (in part), Cochenour Yilgarn: **Golden Mile, Jundee**, Wiluna, Racetrack
Disseminated-stockwork zones	Zones of 5 to 20% sulfides, as uniform disseminations or along foliation-parallel bands, with variably developed stockworks of sulfidic fractures or quartz veinlets, and crackle-type breccias Sulfides are pyrite or arsenopyrite, with molybdenite abundant at Hemlo	Albite-carbonate-sericite-pyrite at greenschist grade Biotite-calc-silicate-pyrrhotite ± pyrite at amphibolite grade K feldspar-muscovite ± calc-silicates at Hemlo	Au > Ag, As, Te, ± W, Hg, Cu, Mo, Sb	Superior: **Malartic, Hemlo, Kerr Addison** (Flow ore), Ross, Beattie, Madsen Yilgarn: **Wallaby, Plutonic, Sons of Gwalia**, Kanowna Belle, Binduli
Sulfide-rich veins and veinlet zones	Sulfide-rich (25–100% sulfide) veins and veinlet zones with intervening disseminated sulfides Sulfides include pyrite, sphalerite, chalcopyrite, and galena	Sericite-chlorite ± chloritoid at greenschist grade Biotite-garnet-cordierite at amphibolite grade	Ag > Au, Cu, Zn, Pb ± As, Te	Superior: **Doyon**, Mouska, Copper Rand, Sleeping Giant Yilgarn: Mount Gibson, Bellevue
Semimassive to massive sulfide lenses	Semimassive to massive sulfide lenses of pyrite, chalcopyrite, sphalerite, and galena, with pyrrhotite and magnetite in some cases	Sericite-quartz ± chlorite or garnet-biotite Quartz-andalusite-kyanite-pyrophyllite	Ag > Au Cu, Zn, Pb, As ± Te, Sb	Superior: **Horne, LaRonde-Penna**, Bousquet 2-Dumagami, Bousquet 1 Yilgarn: none

A5B), which consists of voluminous extensional vein arrays developed within the competent granophyric layer of the subvertical differentiated Golden Mile dolerite sill (Clout et al., 1990).

Sulfidic replacements in banded iron formation: This style of mineralization consists of strata-bound sulfide replacement of iron-rich layers in chert-magnetite BIF, as at Mount Magnet and Musselwhite, or of magnetite-rich graywacke-mudstone, as at McLeod-Cockshutt and in some orebodies at Sunrise Dam (Table 1; Fig. 4C). Sulfidic replacement ores are commonly, but not exclusively, associated with crosscutting quartz-carbonate veins and veinlet zones. Within BIF units, mineralization of this style typically occurs either along the hinges of deposit- to map-scale folds (Musselwhite) or along the intersection with crosscutting structures (Central Patricia, Mount Magnet). At Musselwhite, mineralization consists of zones of pyrrhotite-bearing quartz veins and adjacent extensive pyrrhotite ± arsenopyrite replacements of iron-rich sedimentary rock layers within a mafic volcanic rock sequence (Hall and Rigg, 1986); the best mineralization occurs along a small parasitic anticline on a limb of a tight map-scale syncline transected by a fault subparallel to the fold axial plane. A number of deposits of this style of mineralization in amphibolite-grade rocks of the Southern Cross province of the Yilgarn (e.g., Nevoria) have also been interpreted as Au-bearing skarns on the basis of the ore and calc-silicate alteration mineral assemblages (Mueller et al., 2004).

Sulfidic replacement lodes and crustiform veins: An important, but relatively uncommon, mineralization style consists of lodes that combine varying proportions of crustiform-colloform–textured carbonate-quartz veins and breccias (Fig. 4D) and of sulfidic replacements of the wall rocks (Fig. 4E) or of vein carbonates themselves. Such lodes are distinctly epizonal in character and dominate at Golden Mile (Clout et al., 1990), Jundee (Hall et al., 2003), and Campbell-Red Lake (MacGeehan and Hodgson, 1982). The most common sulfide mineral is pyrite, but arsenopyrite dominates at Campbell-Red Lake, stibnite is locally abundant at Wiluna, and tellurides are a hallmark of the Golden Mile deposit. This type of mineralization is preferentially hosted in mafic rocks and forms extensive lode systems in large deposits such as Golden Mile and Campbell-Red Lake. At the Golden Mile deposit, a network of steeply dipping lodes, known as Fimiston-type lodes, overprints both limbs of the asymmetric, northwest-trending D_1 Kalgoorlie syncline (Fig. A5C). The lodes cut a swarm of upright feldspar porphyry dikes but are, in turn, locally cut by hornblende-rich porphyry dikes (Gauthier et al., 2004) and by extensional quartz-carbonate veins similar to those at the nearby Mount Charlotte deposit (Clout et al., 1990). At the Campbell-Red Lake deposit (Fig. A5D), crustiform carbonate veins and overprinting auriferous sulfidic replacement lodes occur along two main east-southeast–trending fault zones that are parallel to the intense local foliation and to the axial planes of map-scale D_2 folds (Dubé et al., 2004a). The crustiform carbonate veins themselves are folded and partly transposed by the northwest-trending foliation and are cut by a series of postore feldspar porphyry and lamprophyre dikes (Dubé et al., 2004a).

Disseminated-stockwork zones: This style of mineralization is relatively common in both cratons and consists of zones of disseminated sulfides, as fine uniform disseminations (Fig. 4F) or as bands concentrated along foliation planes in highly strained rocks (Fig. 4G), and stockworks of sulfidic fractures or of millimeter- to centimeter-thick quartz veinlets (Table 1). It is also characterized by an absence or a paucity of throughgoing quartz-carbonate veins. This mineralization style dominates at Madsen (Dubé et al., 2004a), Beattie (Robert, 2001), Kanowna Belle (Fig. A5E; Ross et al., 2004), Wallaby (Salier et al., 2004), and Plutonic (Fig. A5F; Rowe et al., 2002). Mineralization of this style shows two main associations. In the first association, disseminated-stockwork–type mineralization is centered on small shallow-level intermediate to felsic porphyry intrusions, many of which were emplaced in clastic sedimentary rocks, i.e., in the upper parts of the stratigraphic column (Kanowna Belle, Wallaby, Binduli, Malartic, Beattie). Such deposits are also well preserved and generally display very low strain. At Kanowna Belle, mineralization is centered on a steeply plunging feldspar porphyry stock and associated dikes that are intruded into conglomerates, grits, and sandstones, along the preexisting high-angle Fitzroy fault (Fig. A5E). In a second association, disseminated-stockwork–type mineralization is confined to mafic rock units and is strata bound (Plutonic, Kerr-Addison flow ore, Sons of Gwalia). Such mineralization occurs in the lower part of the stratigraphic column and, in most cases, the host mafic units are in contact with ultramafic units. At Plutonic, such mineralization occurs as a series of lodes within, and subparallel to, a foliated amphibolite unit between two ultramafic units (Fig. A5F). The lodes have been overprinted by significant strain and display isolated isoclinal hinges and boudins of highly transposed quartz veinlets. The host volcanic rock sequence and the lodes have been folded and cut by a series of thrust and high-angle faults, themselves cut by later auriferous quartz-carbonate veins.

Sulfide-rich veins and veinlet zones: This style of mineralization consists of sulfide-rich (>25% sulfides) through-going veins or associated veinlet zones (Fig. 4H). It is distinct from quartz-carbonate vein-style mineralization in terms of its greater sulfide mineral abundances, the presence of significant base metal sulfides, and the nature of associated alteration (Table 1). This style of mineralization is not common but forms the bulk of mineralization in a few deposits, such as Doyon (Robert and Poulsen, 1997), Sleeping Giant (Gaboury and Daigneault, 1999), and Mount Gibson (Yeats et al., 1996). It is also associated with semimassive to massive sulfide lenses in some deposits (see below).

Semimassive to massive sulfide lenses: A final, but important, gold mineralization style consists of concordant auriferous base metal-rich sulfide lenses (commonly >50% sulfides). This style of gold mineralization is present only in a few deposits in the Superior craton (Horne, Bousquet 2-Dumagami, and La Ronde-Penna), where it combines with sulfide-rich veins and veinlet zones to form deposits that have the hallmarks of typical VMS deposits (Franklin et al., 2005), with the nuances that they are inherently enriched in precious metals (see Robert and Poulsen, 1997). These deposits occur near the top of felsic volcanic rock sequences, particularly in volcaniclastic dacitic to rhyolitic units. Some deposits are highly strained, as is the case at Bousquet 2-Dumagami and LaRonde-Penna, which has partly obscured the discordant nature of the footwall zones of sulfide-rich veins and veinlets

and associated alteration zones (Dubé et al. 2004b). Generally barren, through-going quartz-carbonate veins, although not abundant, overprint the sulfide-rich ores at Bousquet 2-Dumagami and La Ronde-Penna.

Variations among deposits

The significance and causes of the variations in characteristics are multiple and are still the subject of much debate. Proposed explanations include variations in host rock type or in metamorphic grade (Colvine, 1989; Groves et al., 1995), differences in crustal levels of formation (Groves, 1993; Gebre-Mariam et al., 1995), and/or the existence of different deposit styles formed at different times (Robert and Poulsen, 1997; Groves et al., 2003).

With the obvious exception of the massive sulfide and related sulfide veins and veinlet zones, the diverse mineralization styles described above share a number of characteristics, including high Au/Ag ratios, enrichment in As, W, and Te, and sericite-ankerite-pyrite alteration (Table 1). These common characteristics have been used to support the notion that most of these deposits have formed by similar, orogenic processes, with most of the variations attributed to differences in host rocks and crustal levels of formation (Groves et al., 2003; Goldfarb et al., 2005). However, a number of other deposits display unique metal composition and hydrothermal alteration and require an association with different hydrothermal fluids and gold ore-forming processes (Groves et al., 2003). For example, although sharing a setting similar to that of other disseminated-stockwork deposits associated with felsic porphyry intrusions, the Hemlo deposit differs markedly with its K-feldspar-sericite alteration, Au-Mo-As-V-Ba-Te-Hg-Sb metal association (Muir, 2002), and overprinting strain and amphibolite-grade metamorphism (Lin, 2001). Similarly, the Boddington, Troilus, and McIntyre (Cu zone) deposits differ from the disseminated-stockwork style of mineralization with their Au-Cu ± Mo metal association, the Ag-rich composition of the ores, and their general affinities with Phanerozoic magmatic hydrothermal systems (Fraser, 1993; McCuaig et al., 2001).

In addition, there are examples of systematic overprinting of different mineralization styles in a number of deposits, which require the existence of multiple gold mineralization events. These include early Cu-Mo-Au disseminated-stockwork mineralization overprinted by an extensive array of quartz-carbonate veins at Hollinger-McIntyre (Mason and Melnik, 1986); sulfidic replacement lodes and colloform veins overprinted by quartz-carbonate veins at Golden Mile (Clout et al., 1990). There are also many examples where barren, syntectonic, shallowly dipping, extensional quartz-carbonate veins, of the style that make ore in other deposits, overprint disseminated-stockwork ores or massive sulfide-style ores. Examples include Kanowna Belle, some syenite-associated deposits in the Abitibi subprovince (Robert, 2001), and LaRonde-Penna (Mercier-Langevin et al., 2004).

When combined, the above relationships attest to the existence of multiple episodes of gold mineralization within the two cratons, and the involvement of more than one ore-forming process. This, in turn, implies a variety of controls on the location of deposits, a fact that is important to consider in exploration, especially in light of the wide spectrum of characteristics and settings represented among >5 Moz deposits (Table 1).

Timing of Gold Deposit Formation

Establishing the time of formation of gold deposits in the evolution of the host greenstone belts is of considerable importance. This problem has received much attention in the last two decades but, given the significant difficulty in establishing unequivocal relative and absolute ages of deposits, it is still a subject of much debate. Many approaches have been applied to this problem, each with inherent limitations. One approach is to bracket the age of mineralization by dating host rocks and postore rocks by robust methods, such as U-Pb determinations on zircon. The general scarcity of postmineral dikes, and ones suitable for isotopic dating, represents a significant limitation, as does the possibility of zircon inheritance, particularly in the Yilgarn craton (Vielreicher et al., 2003). There is also common difficulty in interpreting the significance of dikes cutting gold mineralization. In several examples in both the Superior and Yilgarn cratons, dikes cut the main stage of mineralization but are themselves hydrothermally altered and may contain gold or be cut by late quartz-carbonate veins (e.g., Hemlo, Kiena, Holloway, Red Lake, Golden Mile, Mount McClure). Such cases can lead to the interpretation of the dikes being synchronous with a protracted mineralization event (e.g., Ropchan et al., 2002), but alternate interpretations could include the existence of a second, unrelated gold mineralization event or that late gold and alteration result from assimilation and contact metamorphism during the emplacement of the postmineral dike (Dubé et al., 2004a).

A second approach is to establish the timing of mineralization with respect to metamorphism and deformation, which in turn may be broadly constrained by regional considerations. There are numerous examples of this approach from the 1980s, carried out before new, more accurate and precise geochronological tools became available. This approach, although potentially valuable, is fraught with difficulties in interpreting whether or not a deposit is deformed and/or metamorphosed in the first place or whether metamorphic fabrics of similar orientation but in different places are time correlative. A third approach has been to directly determine the ages of ore and ore-related minerals, most commonly with ^{40}Ar-^{39}Ar analysis of white mica, fuchsite, biotite, and amphiboles; U-Pb analysis of hydrothermal zircon, rutile, titanite, monazite, and xenotime; and Re-Os analysis of molybdenite, arsenopyrite, and other sulfides. Many of these methods are still in the experimental stage and have yielded mixed results. For example, a number of the determined ^{40}Ar-^{39}Ar ages of mineralization are much younger than can be realistically inferred by the geologic facts and, therefore, must be regarded as minima (Kerrich and Cassidy, 1994). In other cases, however, measured ages fall within the brackets established by the other approaches and, therefore, may provide reasonable estimates of ages of mineralization.

The existing geochronologic constraints on the gold deposits of the main gold belts of the Superior and Yilgarn cratons have been compiled in Figure 5. The inferred ages of mineralization have also been bracketed following the approaches outlined above and only using results of reliable

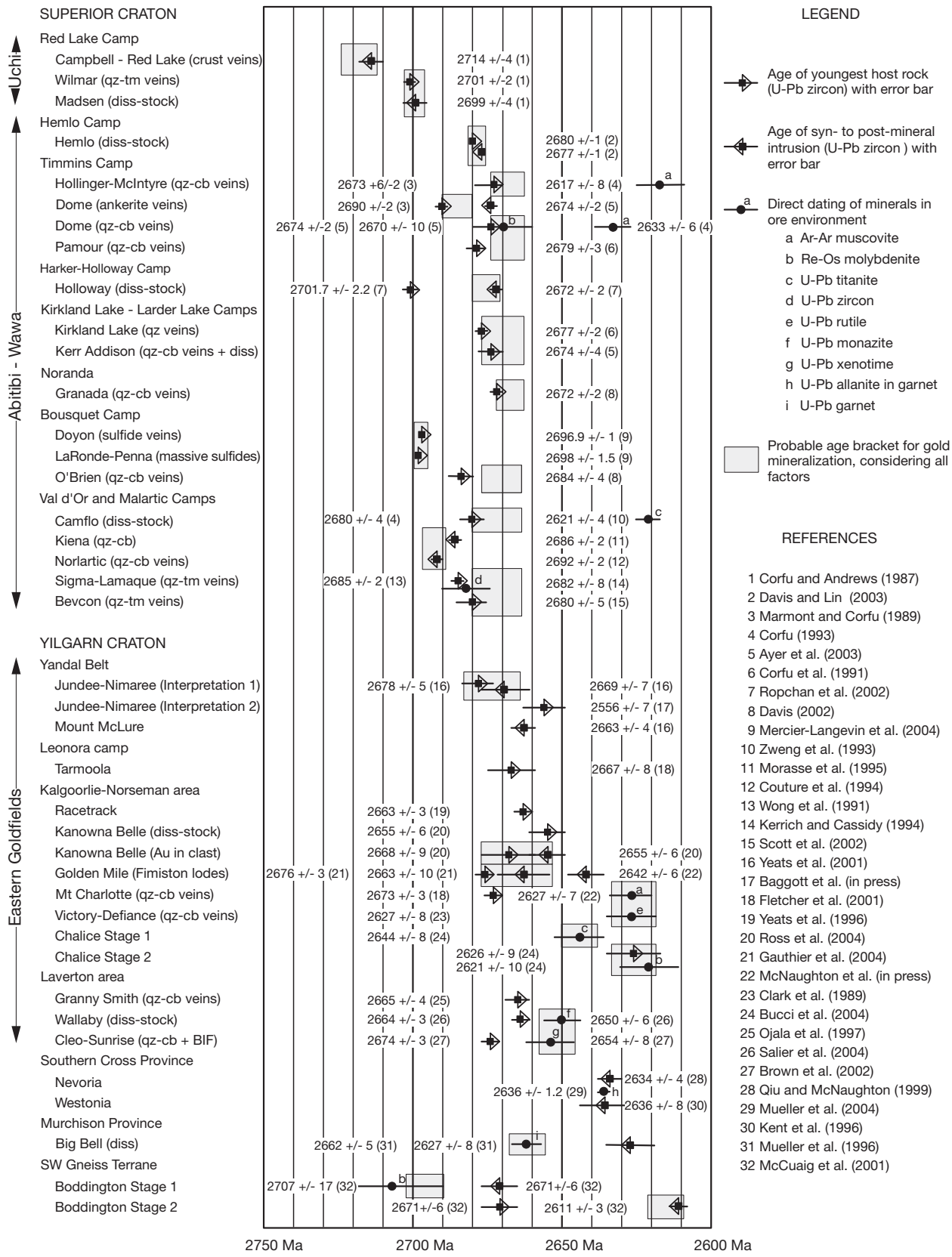

FIG. 5. Compilation of age constraints on selected gold deposits of the Superior and Yilgarn cratons. The indicated probable age brackets for mineralization are based on absolute age constraints and on geologic relationships of mineralization to well-documented deformation events in the respective camps. See text for discussion.

methods. Two major observations results from this compilation. The first is that, although volcanic, plutonic, and sedimentary rocks formed throughout a span of >300 m.y. in both cratons (Fig. 3), most deposits formed during the last 100 m.y. of this interval and the majority of those between 2700 and 2630 Ma. This period coincides with the waning stages of volcanism and general peaks in plutonism and deformation, each of which has been invoked as the main driving process for the formation of gold deposits. The second observation is that within each of the cratons, and even within single camps (Fig. 5), there is not a single clearly identified gold mineralizing event. On the basis of careful field observations and reliable geochronological constraints, there is clear evidence of at least two events in a number of well-documented cases.

In the Red Lake camp of the Rice Lake-Pickle Lake gold belt (Fig. 5), colloform carbonate veins and later sulfidic replacements at the Campbell-Red Lake deposit are both cut by 2714 ± 4 Ma[2] feldspar porphyry dikes (Fig. 5; Dubé et al., 2004a), whereas the quartz-tourmaline veins at the nearby Wilmar deposit are hosted by a 2701 ± 2 Ma granitic intrusion (Fig. 5). A 2699 ± 4 Ma granodiorite dike also cuts the ore at the Madsen deposit (Fig. 5). These constraints indicate two gold events separated by at least 10 m.y., although the presence of colloform vein clasts in the 2747 Ma Huston conglomerate (SHRIMP U-Pb zircon: Dubé et al., 2004a) suggests even longer time interval between the two events. In the Val d'Or camp in the Timmins-Val d'Or gold belt, deformed quartz-carbonate breccia veins in the Norlartic deposit are cut by 2692 ± 2 Ma dikes (Fig. 5), whereas younger quartz-tourmaline veins at the Bevcon deposit cut a 2680 ± 5 Ma pluton (Fig. 5), also pointing to a minimum of about 10 m.y. between the two gold events. The presence of gold-rich VMS deposits in 2698 to 2696 Ma volcanic units of the Blake River Group (Mercier-Langevin et al., 2004) in the Bousquet camp farther to the west adds to the range of ages of gold mineralization in the Timmins-Val d'Or belt (Fig. 5).

In the Kalgoorlie camp of the Wiluna-Norseman gold belt, the age of Fimiston-type lodes is constrained by 2676 ± 3 Ma preore feldspar porphyry dike and a 2663^{+11}_{-9} Ma postore feldspar-hornblende porphyry dike (Fig. 5), although there is evidence that such dikes may contain inherited zircons. A lamprophyre dike from the Oroya shoot, a late Fimiston-type ore shoot noted for its abundant vanadium-muscovite, contains magmatic-hydrothermal zircons with SHRIMP U-Pb ages of 2642 ± 6 Ma (McNaughton et al., in press) and provides a minimum age for Fimiston-type mineralization. Quartz-carbonate veins similar to those at Mount Charlotte cut Fimiston-type lodes (Clout et al., 1990). At the Kanowna Belle deposit, a clast containing a gold-bearing vein within a conglomerate that is intruded by a 2655 ± 6 Ma (SHRIMP U-Pb zircon) mineralized porphyry dike provides further evidence for at least two distinct stages of gold mineralization (Fig. 5). In other segments of the Wiluna-Norseman belt, main-stage gold mineralization at the Chalice deposit has been directly dated at 2644 ± 8 Ma (SHRIMP U-Pb titanite). Minor later mineralization at 2621 ± 10 Ma (Re-Os molydenite) is coeval with the intrusion of gold-bearing monzogranite dikes at 2626 ± 9 Ma (SHRIMP U-Pb zircon; Bucci et al., 2004). Similar ages for gold mineralization were also obtained on hydrothermal monazite (2631 ± 9 Ma; SHRIMP U-Pb: Nyugen, 1997) and rutile (2627 ± 10 Ma: Clark et al., 1989) for the Revenge and Victory orebodies in the St Ives gold camp (Fig. 5).

At the Westonia and Nevoria deposits in the Southern Cross province, postore monzogranite dikes have been dated by SHRIMP U-Pb at 2636 ± 8 and 2634 ± 4 Ma, respectively (Fig. 5). At Westonia, ore-related molybdenite has an Re-Os age of 2640 ± 9 Ma and allanite-bearing garnet at the Nevoria deposit has a TIMS U-Pb age of 2636 ± 2 Ma (Mueller et al., 2004). At the Boddington deposit, crosscutting relationships, extensive U-Pb geochronology on zircon, and Re-Os dating of distinct populations of molybdenite (both paragenetically associated with gold) indicate an early gold introduction event at ~2700 Ma, closely associated with the intrusion of host diorites, and a second period of mineralization at ~2615 Ma, synchronous with emplacement of post-tectonic monzogranites (McCuaig et al., 2001).

There is also evidence that gold mineralization in the Superior and possibly Yilgarn cratons was diachronous. In the Superior craton, the ages of gold mineralization tend to mimic those of terrane accretion from ~2715 Ma in the Uchi subprovince to ~2670 Ma in the Abitibi subprovince (Percival, 2003). In the Yilgarn craton, there is also evidence that, at least for the Eastern Goldfields province, mineralization was diachronous, with mineralization in the Laverton gold belt possibly 10 to 15 m.y. older than mineralization in the Wiluna-Norseman gold belt (Fig. 5; Vielreicher et al., 2003; Blewett et al., 2004). Direct dating of ore-related monazite and xenotime at the Sunrise-Cleo and Wallaby deposits (Fig. 5) gives SHRIMP U-Pb ages of 2654 ± 8 Ma (xenotime) and 2650 ± 6 Ma (monazite).

In summary, there are many well-documented cases where the geologic evidence and absolute dating by reliable methods clearly demonstrate two and even three geologically and temporally distinct gold ore-forming events in individual camps or individual deposits. Dating methods that give results at odds with the geology are mainly associated with minerals that are susceptible to resetting by postmineral structural, thermal, or fluid events, for example ^{40}Ar-^{39}Ar ages of micas and U-Pb ages of rutile (Kerrich and Cassidy, 1994).

Characteristics of Gold Camps

The Kalgoorlie, Timmins, Red Lake, and Laverton gold camps, the largest in each of the four main gold belts, collectively account for nearly one-half of the combined gold endowment of both cratons (Fig. A4). Their geologic attributes at the camp scale are, therefore, of considerable relevance to addressing questions of what, if any, geologic features are specific to well-mineralized gold camps, and what factors lead to the concentration of deposits into camps, and their location within them. The camps are compared through a series of standardized stratigraphic columns (Fig. 6) and geologic maps covering similar areas (Fig. 7A-D), following the approach of Hodgson and MacGeehan (1982).

[2] Reported specific ages are TIMS U-Pb zircon ages unless otherwise specified.

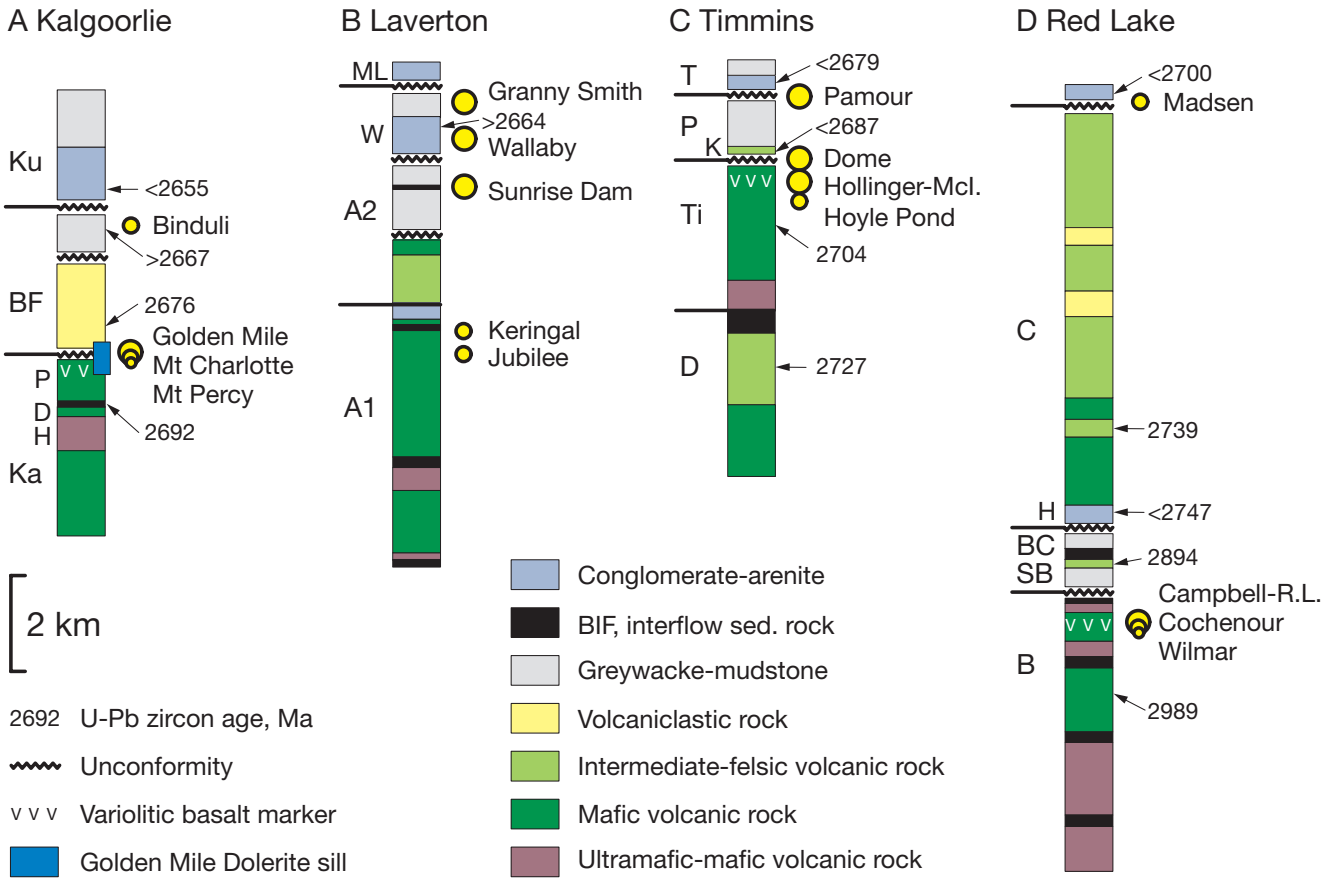

FIG. 6. Simplified stratigraphic columns for the main gold camps in the Superior and Yilgarn cratons. See text for discussion. A. Kalgoorlie, adapted mainly from Krapez et al. (2000). BF = Black Flag Group, Ka = Kambalda Group, Ku = Kurrawang Group, D = Devon Consols basalt, H = Hannan's Lake serpentinite, P = Paringa basalt. B. Laverton, adapted from Hallberg (1985). A1 and A2 = associations 1 and 2 of Hallberg (1985), ML = Mount Lucky conglomerate, W = Wallaby conglomerate. C. Timmins, adapted from Bleeker (1995) and Ayer et al. (2002). D = Deloro Group, K = Krist Formation, P = Porcupine Group, T = Timiskaming Group, Ti = Tisdale Group. D. Red Lake, adapted from Wallace et al. (1986) and Sanborn-Barrie et al. (2001). C. Confederation assemblage. H. Huston conglomerate. B = Balmer assemblage, BC = Bruce Channel assemblage, SB = Slate Bay assemblage.

Kalgoorlie

The Kalgoorlie camp in the Wiluna-Norseman gold belt contains the largest concentration of gold (Fig. A4), with most gold in the Golden Mile deposit (Fig. 7A). The camp straddles the regionally extensive Boulder-Lefroy fault system, represented by the Boulder and Abattoir faults and higher order structures in the Kalgoorlie region (Fig. 7A). The komatiites and basalts of the Kambalda Group are unconformably overlain by the complex Black Flag Group of felsic volcanic, volcaniclastic, and clastic sedimentary rocks, in turn unconformably overlain by coarse clastic sedimentary rocks of the Kurrawang sequence (Fig. 6A). The volcano-sedimentary succession was intruded by a set of fractionated mafic layered sills, including the 800-m-thick, ~2675 Ma Golden Mile dolerite, emplaced near the contact between the Kambalda and Black Flag Groups (Fig. 6A) and the most significant host for gold in the camp (Clout et al., 1990). The volcanic rocks of the Kambalda Group are exposed in a series of north- to northwest-trending structural windows through extensive clastic sedimentary and volcaniclastic rocks of the Black Flag Group (Fig. 7A). Felsic intrusions are not abundant in the district and are mainly limited to porphyry stocks and dikes. Rocks within the camp were affected by early thrusts and by map-scale D_1, D_2, and D_3 folds (Swager, 1989). Resulting features include the (D_1) Kalgoorlie anticline-syncline pair and the Golden Mile fault, themselves overprinted by later large folds, such as the (D_2) Kurrawang syncline and the (D_3) Boomerang anticline, with associated regional north-northwest– and north-trending and subvertical regional foliations, respectively (Swager, 1989). A biotite isograd separates the camp into a lower to middle greenschist facies to the east and an upper greenschist facies to the west (Fig. 7A). Extensive carbonate alteration is present in the camp and envelops the Golden Mile deposit (Fig. A5C; Phillips, 1986).

Gold deposits cluster in the northeast part of the camp, where they are distributed along the Golden Mile fault and Kalgoorlie syncline, and in the southwest, along the eastern limb of the Kurrawang syncline (Fig. 7A). In the northeast cluster, the Mount Charlotte and Golden Mile deposits are hosted by the Golden Mile dolerite, particularly in its upper siliceous and iron-rich members (Fig. A5B, C; Clout et al., 1990). The succession is cut by quartz-feldspar and feldspar-hornblende porphyry dikes, which form swarms within the

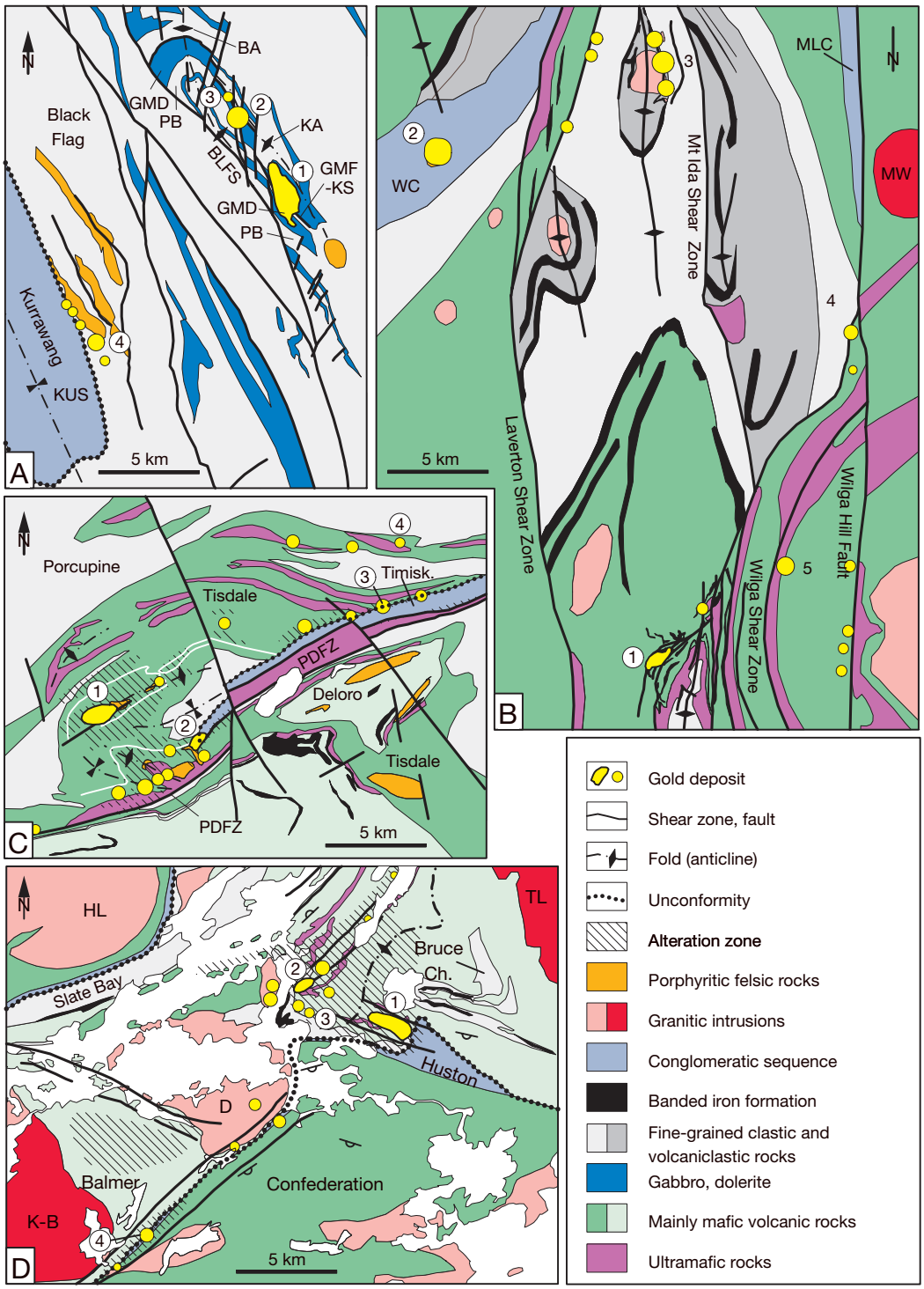

FIG. 7. Simplified geologic map of selected gold camps. A. Kalgoorlie camp, Eastern Goldfields province. Compiled from Keats (1987), Clout et al. (1990), and Mikucki and Roberts (2004). Deposits: 1 = Golden Mile, 2 = Mount Charlotte, 3 = Mount Percy, 4 = Binduli. BA = Boomerang anticline, BLFS = Bouder-Lefroy fault system, GMD = Golden Mile dolerite, GMF = Golden Mile fault, KA = Kalgoorlie anticline, KS = Kalgoorlie syncline, PB = Paringa basalt, KUS = Kurrawang syncline. B. Laverton area. Compiled from Hallberg (1986), Brown et al. (2002), and Salier et al. (2004). Deposits: 1 = Sunrise Dam, 2 = Wallaby, 3 = Granny Smith, 4 = Keringal, 5 = Jubilee. MLC = Mount Lucky conglomerate, MW = Proterozoic Mount Weld carbonatite, WC = Wallaby conglomerate. C. Timmins camp. Adapted from Pyke (1982) and Robert and Poulsen (1997). Deposits: 1 = Hollinger-McIntyre, 2 = Dome, 3 = Pamour, 4 = Hoyle Pond. PDFZ = Porcupine Destor fault zone. White line represents variolitic basalt marker. D. Red Lake camp. Compiled from Dubé et al. (2004) and Sanborn-Barrie et al. (2004). In addition to mafic volcanic rocks, the Confederation assemblage contains significant volumes of rocks of intermediate composition. Deposits: 1 = Campbell-Red Lake, 2 = Cochenour, 3 = Wilmar, 4 = Madsen. D. Dome stock, HL = Hamill Lake batholith, K-B = Killala-Baird batholith, TL = Trout Lake batholith.

Golden Mile and Mount Percy deposits. In the southwest cluster, the Binduli and associated deposits occupy a significantly different setting and are hosted by coarse clastic and epiclastic rocks of the Black Flag Group (Krapez et al., 2000) that are cut by felsic porphyry stocks and dikes in the vicinity of the Kurrawang syncline (Figs. 6A, 7A).

There are several distinct styles of mineralization in the camp and three in the Golden Mile deposit itself. First, and most significant, are Fimiston-type sulfidic replacement lodes and associated crustiform carbonate-quartz-anhydrite veins and breccias of the Golden Mile deposit (Clout et al., 1990). Commonly portrayed as occupying shear zones (Boulter et al., 1987), they are actually narrow, but continuous, tabular lodes (Fig. A5C) surrounded by carbonate-sericite-albite-pyrite alteration zones, which themselves commonly display two metamorphic foliations correlated with regional D_2 and/or D_3 events (Boulter et al. 1987; Gauthier et al., 2004). A second style of mineralization consists of volcanic rock-hosted, strata-bound, disseminated sulfide-rich lodes, such as the Oroya Shoot at the Golden Mile deposit, which is slightly younger but likely related to the Fimiston-type lodes (Bateman and Hagemann, 2004). A third and yet younger stage of mineralization, known as Mount Charlotte-type, dominates at the Mount Percy and Mount Charlotte (Fig. A5B) deposits and consists of extensional quartz-carbonate vein arrays that locally overprint the older Fimiston-type lodes (Clout et al., 1990). Finally, disseminated-stockwork-style mineralizaton at Binduli occurs in sericitized and carbonatized sandstone, conglomerate, and felsic porphyry, a host-rock setting that resembles that of the Kanowna Belle deposit (Fig. A5E). The relationship of this style of mineralization to the others has not been established.

The age and origin of the gold deposits in the Kalgoorlie camp are controversial. There is a general agreement that Mount Charlotte-type quartz-carbonate veins have formed syntectonically, during D_3 or younger deformation, consistent with the above age constraints (Fig. 5), and thus represent synorogenic mineralization. The Golden Mile deposit has been interpreted as a late mesozonal orogenic deposit (Groves et al., 1998), as an early (pre-D_2) epi- to mesozonal orogenic deposit (Bateman and Hagemann, 2004), or as an early gold-telluride epithermal deposit (Clout, 1989). The last two interpretations are more consistent with the epizonal character of the Fimiston-type lodes and their overprinting by north-northwest–trending D_2 regional foliation and reverse shear zones (Bateman and Hagemann, 2004).

Laverton

The Laverton area, with its Wallaby-Granny Smith and Sunrise Dam camps, has emerged as a significant gold-producing region (Fig. 7B). Both camps occur within the Laverton tectonic zone (Hallberg, 1986), a 10- to 25-km-wide, north-south–striking corridor occupied mainly by folded felsic to intermediate volcanic and volcaniclastic sedimentary rocks with local BIF (Fig. 7B). The dominantly mafic and ultramafic volcanic rocks to the west and east of this corridor comprise "association 1" and "association 2" of Hallberg (1986), interpreted as the lower and upper parts, respectively, of a regionally extensive volcanic rock sequence (Fig. 6B). Clastic and epiclastic sandstone, siltstone, and tuff, with locally interbedded BIF, make up the majority rocks within the corridor (Fig. 7B) and represent the upper parts of the 2715 to 2705 Ma association 2 (Brown et al., 2001). These sequences are in turn unconformably overlain by narrow belts of <2675 Ma polymictic conglomerate and sandstone along the western and eastern edges of the Laverton corridor (Fig. 7B). The Laverton corridor is marked by a network of anastomosing shear zones, particularly by the bounding Laverton and Wilga shear zones, which, along with north-trending antiforms, define the overall structure of the area (Fig. 7B), are generally ascribed to regional D_2 shortening (Ojala et al., 1997; Davis, in press). Clusters of small granitoid intrusions are coincident with both gold camps. These intrusions range from 2675 to 2663 Ma (Fig. 5; Ojala et al., 1997; Brown et al., 2002; Salier et al., 2004), providing minimum ages for the supracrustal rocks they intrude. Contact metamorphic aureoles excluded, the rocks of this area display mainly greenschist-facies mineral assemblages, although Hallberg (1986) noted common subgreenschist-facies rocks along the central part of the Laverton corridor.

The gold deposits cluster in the Wallaby-Granny Smith and the Sunrise Dam camps (Fig. 7B). Although the smaller deposits, such as Keringal and Jubilee, are located in the mafic-ultramafic rock portion of the stratigraphic column, the larger Granny Smith, Sunrise Dam, and Wallaby deposits are all hosted in clastic and epiclastic rocks in the upper part of the column (Fig. 6B), where they are also associated with anticlinal structures. In addition, all of the deposits display a notable spatial association with preore felsic intrusive rocks (Ojala et al., 1997; Brown et al., 2002; Salier et al., 2004).

The deposits also display considerable diversity in styles of mineralization. At Sunrise Dam, mineralization is hosted in a folded package of intermediate volcaniclastic sedimentary rocks and BIF cut by an array of 2674 ± 3 Ma preore rhyodacite porphyry dikes (Brown et al., 2002). Ore styles include low-grade zones of disseminated sulfides and quartz-carbonate veinlets in gently dipping shear zones and in surrounding BIF, and high-grade, steeply dipping, narrow quartz-carbonate-pyrite veins transverse to the shears, both with associated sericite-carbonate alteration. The Wallaby deposit, centered on a 2664 ± 3 Ma monzonite-syenite stock and dike complex intruding polymictic conglomerates (Salier et al., 2004), consists of disseminated-stockwork-style mineralization and subordinate carbonate-quartz veinlets (Fig. 4F), with associated dolomite-albite-pyrite alteration, overprinting a steeply plunging, pipelike body of actinolite-magnetite-calcite alteration surrounding the intrusive complex (Salier et al., 2004). Quartz-carbonate vein-style mineralization characterizes the Granny Smith and the Jubilee deposits. At Granny Smith, an array of quartz-ankerite veins is associated with a moderately dipping, reverse fault along the contact between granodiorite and fine-grained clastic sedimentary rocks and is accompanied by vein-scale sericite-ankerite-pyrite alteration (Ojala et al., 1997). The contact metamorphic aureole surrounding the intrusion is also overprinted by the veins and associated alteration.

Despite the strong empirical correlation between gold and felsic intrusions, detailed studies suggest that the association may not be a direct genetic one but rather attributable to rheological contrasts between the intrusions and their hosts

(Ojala et al., 1993; Brown et al., 2002; Salier et al., 2004). In all cases, there is paragenetic evidence to suggest the sericite-carbonate alteration related to gold mineralization overprints the intrusions and their contact metamorphic and/or metasomatic products, but it is difficult to establish whether this represents the natural evolution of intrusion-related gold systems or rather the overprinting by distinctly different orogenic processes (Salier et al., 2004). Geochronological studies in these camps demonstrate that felsic plutons of a wide range of compositions were emplaced between 2674 and 2664 Ma, and suggest that gold mineralization may significantly postdate the intrusions but is unlikely younger than 2650 Ma (Fig. 5).

Timmins

The Timmins camp in the Timmins-Val d'Or gold belt is located immediately north of the Porcupine-Destor regional fault zone, which juxtaposes lower parts of the stratigraphic column in the southeast with the upper part of the column in the northwest (Figs. 6C, 7C). One of the major features of the camp is the presence of two folded angular unconformities. The older occurs at the base of rocks of the Porcupine Group, with the volcanic rocks of the 2690 to 2687 Ma Krist Formation at its base. The younger unconformity occurs at the base of the conglomerate, graywacke, and slate units of the Timiskaming Group and is dated at <2679 ± 2 Ma (Fig. 6C; Corfu, 1993; Ayer et al., 2003). Rocks of the Porcupine and Timiskaming groups overlie the 2727 to 2698 Ma tholeiites and komatiites of the Tisdale and Deloro groups. Rocks in the camp are overprinted by a weak to moderate, subvertical foliation that strikes east-northeast and by a strong, moderately easterly plunging lineation (Pyke, 1982). North of the Porcupine-Destor fault zone, east-trending (D_1) folds of rocks of the Porcupine and Tisdale groups predate the Timiskaming unconformity (Hodgson et al., 1990; Bleeker, 1995) and themselves overprint earlier northwest-trending (pre-D_1) folds (Fig. 7C). The unconformity and rocks of the Timiskaming Group have been folded into a northeast-trending (D_2) syncline truncated by the Porcupine-Destor fault zone (Bleeker, 1995). North of this fault zone, the overall structure is that of a central window of volcanic rocks of the Tisdale Group within a larger mass of rocks of the Porcupine Group, whereas a structural dome exposes mainly rocks of the stratigraphically lower Deloro Group to the south (Fig. 7C). Quartz-feldspar porphyry stocks of the same age as volcanic rocks of the Krist Formation are present in the camp and form important clusters near the Hollinger-McIntyre and Dome deposits (Fig. 7C). Rocks in the Timmins camp have been overprinted by lower greenschist-grade metamorphism, with a few localized areas of upper greenschist assemblages, particularly in the vicinity of the Dome and Hollinger-McIntyre deposits (Thompson, 2004).

Four main deposit clusters include those centered in the Hollinger-McIntyre, Dome, Pamour, and Hoyle Pond deposits (Fig. 7C). All of these clusters, except the Hoyle Pond cluster, are surrounded by extensive carbonate alteration zones. Most gold deposits are hosted in high Fe tholeiitic basalts near the top of the volcanic rock sequence (Hollinger-McIntyre, Hoyle Pond, most ore at Dome) and the lowermost strata of the Timiskaming Group (significant ore at Dome-Paymaster and Pamour; Fig. 6C).

Quartz-carbonate veins and vein arrays make up the most significant style of mineralization in the Timmins camp. At the Hollinger-McIntyre deposit, a 2-km^2 array of quartz-ankerite veins is present mainly west of the Pearl Lake porphyry stock (Fig. 7C) and overprints Cu-Mo-Au disseminated-stockwork–style mineralization associated with the porphyry stock (Davies and Luhta, 1978; Mason and Melnik, 1986). At the Pamour deposit, which straddles the Timiskaming unconformity to depths of >1.5 km, the bulk of the ore consists of zones of sheeted quartz-carbonate veins and disseminated sulfides in adjacent wall rocks, accompanied by extensive laminated quartz veins in moderately to steeply dipping reverse shear zones (Price and Bray, 1948). The Dome deposit comprises several styles of mineralization in volcanic, intrusive, and sedimentary rocks, over an area of 2.7 by 1.2 km (Rogers, 1982). Gold-bearing quartz-carbonate veins occur as discordant, laminated veins in volcanic rocks, and as extensional vein arrays that also cut porphyry stocks and sedimentary rocks of the Timiskaming Group. Concordant crustiform ankerite veins along interflow sedimentary units in volcanic rocks represent an important style of mineralization where they are overprinted by later extensional quartz-tourmaline veins. Zones of disseminated sulfide mineralization, consisting of 2 to 10 vol percent pyrite and pyrrhotite with or without associated extensional vein arrays, forms another style of mineralization that is best developed in porphyry stocks and sedimentary rocks of the Timiskaming Group (Proudlove et al., 1989).

The bulk of gold mineralization in the Timmins camp, represented by quartz-carbonate veins and vein arrays, is of relatively late timing, given that such veins cut the <2679 ± 2 Ma sedimentary rocks of the Timiskaming Group at the Dome and Pamour deposits, and cut a 2673^{+6}_{-2} Ma albitite dike at the Hollinger-McIntyre deposit (Fig. 5; Corfu, 1993). However, there is also evidence for earlier hydrothermal events. The concordant crustiform ankerite veins at Dome, of the same crustiform vein style of mineralization as at Red Lake, are the product of an early hydrothermal event, based on their occurrence as clasts in the basal conglomerate of the Timiskaming Group (Dubé et al., 2003). The presence of auriferous sulfide clasts in the conglomerate at the Dome and Pamour deposits may represent an even earlier gold mineralizing event (Gray and Hutchinson, 2001), although uncertainties remain about the timing of gold introduction into the clasts (pre- or postsedimentation?).

Red Lake

The Red Lake camp in the Rice Lake-Pickle Lake gold belt is marked by an abundance of Mesoarchean rocks, some of which are significant hosts to gold mineralization (Figs. 6D, 7D). The greenstone succession is dominated by the 2990 to 2894 Ma rocks of the Balmer and Bruce Channel groups (Fig. 6D; Sanborn-Barrie et al., 2001) and is unconformably overlain by the <2750 Ma mafic to felsic volcanic rocks of the Confederation Group. A conglomerate unit locally marks the angular unconformity at the base of the Neoarchean sequence (Fig. 7D), and another conglomerate unit near the Madsen deposit, dated at <2700 ± 6 Ma (Sanborn-Barrie et al., 2004), suggests the presence of another, younger unconformity (Fig. 6D). The structure of the camp is dominated by

a northeast-trending anticlinorium, generally attributed to D_1, cored by Mesoarchean rocks and flanked by Neoarchean rocks (Fig. 7D). The anticlinorium is cut by the Kilalla-Baird intrusion in the southwest and the Walsh Lake intrusion in the northeast, both emplaced at approximately 2700 Ma. Early (pre-D_1) Mesoarchean folds are truncated by the unconformity at the base of the Confederation Group. Map-scale east- to east-southeast–trending D_2 folds are best developed in the northeastern part of the camp (Fig. 7D; Sanborn-Barrie et al., 2004). These D_2 folds are accompanied by a regional steeply dipping foliation, which locally intensifies to define a high-strain zone at the Campbell-Red Lake deposit (Andrews et al., 1986). Late D_3 deformation is recorded by crenulation cleavages and brittle-ductile to brittle faults. Although high-strain zones are present in the camp (Andrews et al., 1986), no major through-going structure has been identified at Red Lake. Although stratigraphically anticlinal, the northeast-trending arch is the locus of low-grade metamorphism, flanked by areas of amphibolite-grade metamorphism (App. Fig. A6). Metamorphism has commonly been attributed to emplacement of the ~2700 Ma Killala-Baird batholith and the Walsh Lake pluton (e.g., Andrews et al., 1986), but recent studies (Thompson, 2003) suggest that the intrusions actually cut metamorphic isograds. Extensive regions of carbonate alteration occur in areas of greenschist-grade rocks near the Madsen deposit and in the area of the Couchenor and Campbell-Red Lake deposits, whereas calc-silicate and alumino-silicate alteration zones have been noted in areas of amphibolite-grade rocks (Fig. A6).

Gold deposits of the Red Lake camp cluster in two main areas along the folded boundary between the Mesoarchean and Neoarchean volcanic rock packages and within extensive carbonate alteration zones (Figs. 6D, 7D). In the northern cluster, the Campbell-Red Lake deposit occurs in a sequence of high Fe tholeiitic, komatiitic, and minor felsic volcanic rocks, near their folded contact with a sequence of younger chemical and clastic sedimentary rocks to the east (Figs. 7D, A5D). These rocks are overprinted by a strong northwest-trending D_2 penetrative foliation (Andrews et al., 1986). Mineralization occurs mainly along two major foliation-parallel fault zones, over a strike length of 2 km, along which orebodies consist of crustiform carbonate veins and associated siliceous-sulfidic replacements, and of disseminated sulfides zones in folded interflow sedimentary units as in the East South C zone (MacGeehan and Hodgson, 1982). In the southern deposit cluster, mineralization occurs along a northeast-trending, high-strain, and highly altered zone that straddles the unconformity between rocks of the Balmer and Confederation Groups (Fig. 7D). The dominant style of mineralization, represented by that at the Madsen deposit, consists of disseminated-stockwork sulfides associated with calc-silicate (diopside-garnet-actinolite-epidote) and aluminous (andalusite-cordierite-staurolite) wall-rock alteration developed in clastic volcanic rocks, conglomerate, and basalt flows (Dubé et al., 2004a). The granodiorite-hosted quartz-tourmaline veins of the small Wilmar and Buffalo deposits (Fig. 7D) represent another, less significant style of mineralization.

The timings and origins of the gold deposits in the Red Lake camp remain controversial. Quartz-tourmaline veins are generally accepted as syn- to late-tectonic, i.e., synorogenic, because they cut the 2701 ± 2 Ma granodiorite at the Wilmar deposit (Fig. 5). However, the large Campbell-Red Lake deposit has been interpreted as a deformed and metamorphosed epithermal deposit (Penzak and Mason, 1999) or alternatively as a syntectonic and synmetamorphic deposit, synchronous with the emplacement of nearby batholiths (Andrews et al., 1986). However, the weight of geologic evidence requires a multistage origin for the deposit (MacGeehan and Hodgson, 1982; Dubé et al., 2004a), with paragenetically early carbonate alteration and auriferous colloform-crustiform carbonate veins overprinted by high-grade siliceous-sulfidic replacements, either prior to or during their ductile deformation and metamorphism (Dubé et al., 2004a). The epizonal character and early timing of much of this deposit is supported by the aluminous character of the alteration, the distinct As-Sb-Zn(-Hg) metal association (MacGeehan and Hodgson, 1982), and by the occurrence of clasts of crustiform carbonate vein in a 2747 Ma conglomerate unit to the southeast of the deposit (Dubé et al., 2004a). The epizonal character of the deposit is not compatible with the upper greenschist to lower amphibolite metamorphism of the host rocks, which requires that they represent two distinct events. A postore feldspar porphyry dike that cuts the siliceous-sulfidic replacement-style mineralization indicates a minimum age of 2714 ± 4 Ma for the deposit (Fig. 5).

Comparison among gold camps

The camps considered above display a number of geologic features that are empirically associated with large gold deposits and that can be regarded as favorable for the development of the deposits. All camps display elements of an anticlinorial structure and show a regional contact, in part unconformable, between mafic-ultramafic volcanic rocks and overlying, commonly coarse, clastic sedimentary rocks. Another feature is the presence of high Fe tholeiites in the local volcanic rock sequence (Fig. 6). Such rocks are not abundant in greenstone belts in general, and their presence in the large gold camps is notable but of unclear significance. Felsic and intermediate porphyries, in the form of stocks or clusters of dikes, are present and intimately associated with gold deposits in all camps. Each camp is also characterized by the presence of multiple styles of gold mineralization, with multiple ages of mineralization clearly documented at Timmins, Kalgoorlie, and Red Lake (Fig. 5). Finally, many large deposits occur stratigraphically near the unconformable contact between mafic-ultramafic rock sequences and overlying coarse clastic sedimentary rocks, typically containing polymictic conglomerates (Fig. 6). The metamorphic grades and the ages of host rocks appear to be unimportant, as they vary significantly among the camps.

However, the above camp-scale characteristics are not exclusively restricted to the best-endowed camps, as they are also documented in camps with much lower gold endowment. Notable examples include the well-explored Chibougamau (95 t Au) and Matachewan (33 t Au) camps in the Superior craton (Fig. 1), and the Agnew-Lawlers (235 t Au), Coolgardie (105 t Au), and Kurnalpi (43 t Au) camps in the Yilgarn craton (Fig. 2). Such differences in gold content of geologically similar camps perhaps reflect differences in gold enrichment of the respective source areas.

Characteristics of Gold Belts

Key metallogenic questions at the belt scale are the following: what distinguishes these gold belts from other areas in these cratons and what factors determine the specific location of the gold camps along them. These questions are addressed by reviewing the geologic characteristics of the two most important gold belts in each craton, as previously identified.

Wiluna-Norseman gold belt

The Wiluna-Norseman belt is defined by numerous gold deposits and camps along a relatively narrow corridor (<75 km) over a strike length of about 1,000 km, with a central, nearly barren segment dominated by granitoid rocks (Figs. 2, 8). This gold belt occupies the central part of the Kalgoorlie terrane, which is bounded by a major fault system to the west and to the east (Fig. 8; Swager, 1997). The gold belt itself is characterized by the north-south persistence of a stratigraphic section similar to that present in Kalgoorlie camp (Fig. 6A), where 2720 to 2660 Ma ultramafic-mafic volcanic, felsic volcaniclastic, and sedimentary rocks dominate (Figs. 8, 9; Swager, 1997; Krapez et al., 2000). These rocks are unconformably overlain by coarse clastic sedimentary rock sequences preserved as narrow belts along some of the regional faults (Figs. 6A, 8; Krapez et al., 2000).

A distinctive feature of this gold belt is the abundance of ultramafic rocks, including komatiites in the lower part of the Kambalda Group, which host world-class nickel ore deposits (Swager, 1997). The gold belt is also the site of some of the youngest volcanic rocks of the craton, represented by ~2665 to 2660 Ma andesitic volcanic and volcaniclastic rocks in the lower part of the Black Flag Group (Krapez et al., 2000). The belt is also marked by large volumes of volcaniclastic and fine-grained clastic sedimentary rocks of the upper parts of the Black Flag Group. In the Norseman, Leonora, and Wiluna areas, 2950 to 2750 Ma volcanic rocks form local basement to 2720 to 2660 Ma volcanic rock sequences (Krapez et al., 2000; Cassidy and Champion, 2004). Common older inherited zircons in volcanic rocks and contamination of many mafic volcanic rocks by sialic crust suggest an ensialic environment of deposition (Campbell and Hill, 1988; Nelson, 1997).

Granitoid intrusions exposed along the gold belt display a wide range of age (Fig. 9) and composition. They include high high-field-strength element granitic rocks closely associated with rhyolitic volcanic rock sequences, high Ca and mafic granite suites overlapping with late stages of felsic volcanism, sedimentation, and regional deformation, with the youngest mafic granites emplaced at ~2655 Ma, and low Ca granitoids emplaced mainly between 2650 and 2640 Ma (Champion and Sheraton, 1997; Champion and Cassidy, 2002). Mafic granites, porphyry dike swarms, and calc-alkaline lamprophyres (Perring et al., 1989) are spatially associated with major fault systems, particularly the Bardoc shear zone and Boulder-Lefroy fault system, and with gold mineralization, such as at the Kanowna Belle deposit and in the St Ives district.

Rocks of the Wiluna-Norseman belt have been regionally metamorphosed from subgreenschist- to upper amphibolite-facies assemblages (App. Fig. A7; Binns et al., 1976; Mikucki

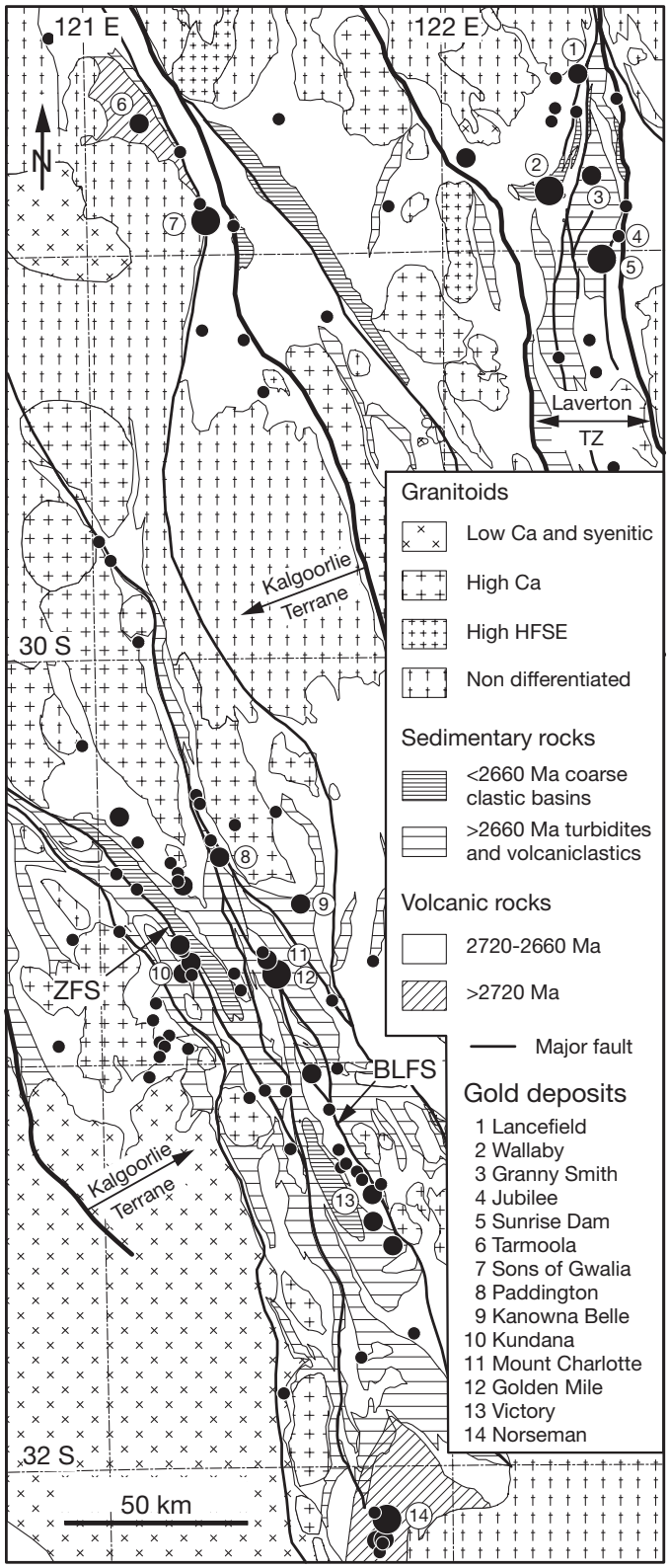

FIG. 8. Geologic map of the south-central Eastern Goldfields province, showing parts of the Wiluna-Norseman (lower half) and the Laverton (top right) gold belts. Compiled mainly from Hallberg (1986), Swager (1997), and GSWA (2005).

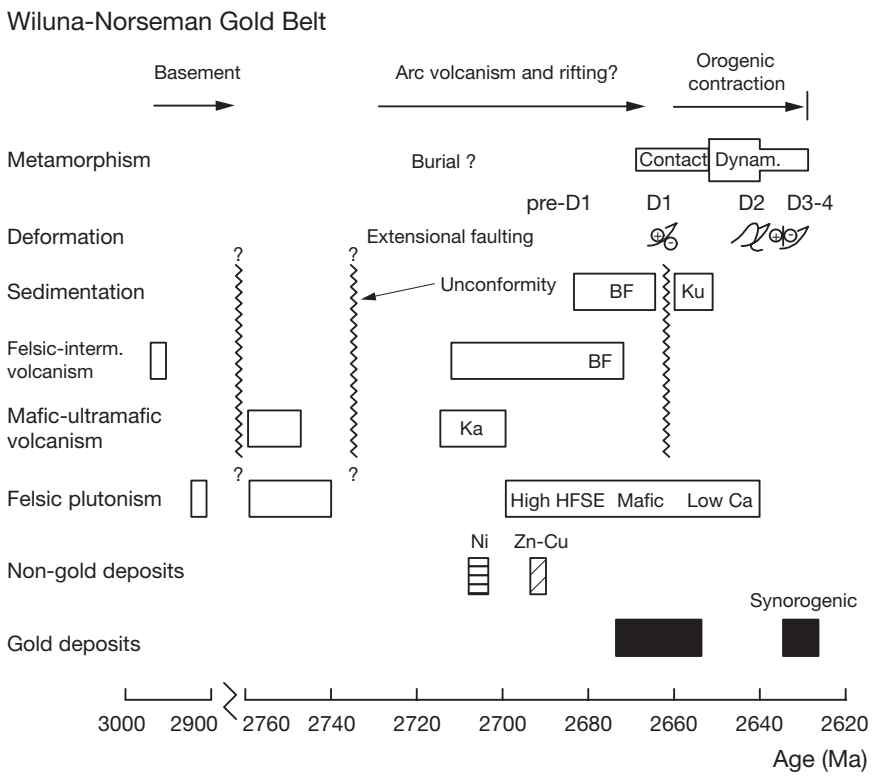

FIG. 9. Tectonic and metallogenic evolution diagram for Wiluna-Norseman belt. Data from Myers (1995), Nelson (1997), Krapez et al. (2000), and relevant references cited in Figure 5.

and Roberts, 2004). Prehnite-pumpellyite-facies assemblages occur in the Wiluna area and east of Kalgoorlie, whereas amphibolite-facies assemblages tend to dominate in the Coolgardie-Norseman district (Fig. A7). The metamorphic history is unclear and involves both dynamothermal metamorphism, recorded by regional penetrative foliation and overprinting the <2655 Ma late-stage clastic sedimentary sequences (Krapez et al., 2000), and isograds that appear to be related to the emplacement of large granitoid intrusions (Fig. A7).

Deformation of the rocks in this gold belt records the superposition of several events (Swager, 1997; Weinberg et al., 2003). The main phase of crustal shortening overprinted the late-stage clastic sedimentary sequences and produced D_2 north-northwest–trending, subvertical cleavage and shallowly plunging regional folds and is thought to coincide with the peak of regional dynamothermal metamorphism. This was followed by phase of transcurrent deformation, which produced sinistral, north-northwest–trending D_3 shear zones and related north-trending folds (Swager, 1997; Weinberg et al., 2003). There is also clear evidence for a phase of D_1 upright folding prior to deposition of the clastic sedimentary rocks, such as the Kalgoorlie anticline-syncline pair (Fig. 7A) and for earlier subhorizontal shear zones, interpreted either as thrusts or detachments, generally with transport directions from south to north (Williams and Currie, 1993; Swager, 1997). The Wiluna-Norseman gold belt also contains a number of internal, first-order regional fault zones, represented by the Boulder-Lefroy and Zuleika fault systems (Fig. 8), in addition to those bounding the Kalgoorlie terrane but external to the gold belt. All of these regional fault zones exhibit complex kinematic histories and contain fabrics that are generally ascribed to the regional D_2 to D_3 shortening events (Weinberg et al., 2003).

Early tectonic models for the Wiluna-Norseman belt, and the Eastern Goldfields province in general, invoked Neoarchean rifting of older Archean crust (Groves and Batt, 1984). More recent plate tectonic models involve accretion of arcs and oceanic crustal fragments along a convergent margin (Barley et al., 1989) or incorporate mantle plume evolution with convergent margin tectonics (Myers, 1995; Barley et al., 1998). Consideration of the autochthonous nature of the greenstone sequences on rifted sialic crust, and subsequent amalgamation of the Kalgoorlie terrane with arc-related terranes to the east, have also resulted in hybrid models for the Eastern Goldfields (Cassidy and Champion, 2004).

Despite a very wide distribution of gold occurrences in the Wiluna-Norseman gold belt, the significant deposits show a close spatial association with specific regional fault zones, along which the deposits clearly cluster into camps (Fig. 8). The bulk of the deposits are located in the southern segment of the belt, particularly along the Boulder-Lefroy fault system, along which camps are separated by distances of 30 to 40 km (Weinberg et al., 2004). Mineralization is hosted in a variety of lithologies, although fractionated mafic intrusions host many of the large deposits. Several styles of mineralization are represented in the belt, including the dominant quartz-carbonate veins (Norseman, Coolgardie, Victory-Revenge, Mount Charlotte, and Tarmoola), epizonal crustiform vein and sulfidic replacement lodes (Golden Mile, Wiluna, and Jundee), and disseminated-stockwork mineralization of both

felsic (Kanowna Belle and Thunderbox) and mafic (Sons of Gwalia and Redeemer) rock associations. There is also clear evidence of more than one gold event in the belt, with significant amounts of gold likely deposited at ~2660 to 2650 Ma and more gold deposited after 2640 Ma (Figs. 5, 9).

Laverton gold belt

The Laverton gold belt forms a narrow (<50-km) belt of significant gold deposits over a strike length in excess of 200 km (Figs. 2, 8). This belt, generally coincident with the Laverton tectonic zone (Hallberg, 1986), forms a north-trending corridor of complex geology and subparallel shear zones that straddle the boundaries between several north-northwest–trending terranes (Fig. 2; Swager, 1997).

Three stratigraphic sequences are recognized in the Laverton region (Fig. 6B; Hallberg, 1985; Brown et al., 2001). Association 1, stratigraphically the lowest, comprises mostly tholeiitic basalt, high Mg basalt, komatiite, BIF, and quartzofeldspathic sandstone (Hallberg, 1985; Myers, 1997). The age of rocks of association 1 is poorly constrained, but this sequence forms an autochthonous basement to the <2715 Ma rocks of association 2. Association 2 is characterized by intermediate volcanic rocks (~2715–2700 Ma) and associated feldspathic volcanogenic sandstone and iron-rich sedimentary rocks, pillowed tholeiites, and minor high Mg basalt (Fig. 6B). Rocks of associations 1 and 2 are unconformably overlain by coarse clastic sedimentary rocks rocks (e.g., Mount Lucky, Lancefield, and Wallaby) that represent the youngest sequences in the Laverton gold belt (Hallberg, 1985; Blewett et al., 2004). The age of these coarse clastic sedimentary rocks is bracketed between ~2665 and 2655 Ma by detrital zircons and small crosscutting intrusions (Nelson, 1997; Salier et al., 2004). Volcanic and sedimentary rocks of the Laverton gold belt are intruded by granite suites similar to those intruding the other parts of the Eastern Goldfields province, including voluminous high Ca granites (~2680-2660 Ma) and abundant mafic granites and porphyry dike swarms. Small syenitic granites are relatively abundant and are spatially associated with major deformation zones. Syn- to late-tectonic, low Ca granites occur throughout the belt, particularly along its margins. Both syenitic and low Ca granites have similar ages that range from ~2655 to 2640 Ma (Nelson, 1997; Champion and Cassidy, 2002).

Metamorphic grades in the Laverton gold belt are typically lower greenschist facies (Binns et al., 1976; Swager, 1997), although amphibolite-facies assemblages tend to be common adjacent to the greenstone-granite contact surrounding the Margaret antiform (e.g., Windarra area; Fig. A7). As was the case for the Wiluna-Norseman belt, the timing of metamorphism is uncertain but is likely <2665 Ma, given that young sedimentary rock sequences, such as those at the Granny Smith and Wallaby deposits, record regional penetrative foliations and display similar metamorphic assemblages to surrounding greenstones.

Several generations of contractional structures are superimposed in the Laverton belt, as was noted in the Wiluna-Norseman belt (Swager, 1997; Newton et al., 2002; Davis, in press). The most prominent structures are north-northwest–trending, shallowly plunging D_2 folds (e.g., Margaret antiform) and associated subvertical cleavage, and D_3 sinistral, north-northwest–trending shear zones and related upright folds that overprint all supracrustal rocks in the belt (Swager, 1997; Blewett et al., 2004; Davis, in press). The D_2 to D_3 structures result from east-northeast to west-southwest crustal shortening that probably marks the onset of a major orogeny. North-trending shear zones that disrupt the regional north-northwest structural grain and control the distribution of several gold deposits (Fig. 8) were also probably produced during this period. Earlier contractional deformation is recorded by the local presence of (D_1) recumbent folds and low-angle thrusts, as well as possible thrust duplexes (Newton et al., 2002). Low-angle ductile shear zones are present in several major deposits in the belt and are common hosts to gold mineralization (Newton et al., 2002); their tectonic significance and timing remain unclear.

Tectonic models for this area generally invoke accretion of arcs and crustal fragments along a convergent margin, with this complex boundary separating terranes with different basement lithological units (Barley et al., 1998; Brown et al., 2001). This interpretation is consistent with differences in xenocrystic and detrital zircon populations in felsic magmatic and sedimentary rocks, respectively (Cassidy and Champion, 2004). Accordingly, the early geologic evolution of the Laverton gold belt is clearly distinct from that of the Wiluna-Norseman gold belt.

Within the Laverton gold belt, a majority of deposits are spatially associated with north-trending shear zones, along which the significant camps and deposits are separated by distances of 30 to 40 km (Fig. 8). The most significant gold deposits of the belt are hosted in clastic sedimentary rock sequences (Wallaby, Sunrise Dam, Granny Smith); others are hosted in mafic-ultramafic rock sequences (Lancefield, Jubilee). As indicated above, mineralization styles include disseminated sulfide-stockwork zones of felsic association at Wallaby, quartz-carbonate veins at Granny Smith and Jubilee, and a mixture of BIF-hosted replacement and quartz-carbonate vein styles at Sunrise Dam. The bulk of the gold mineralization at Wallaby and Sunrise Dam is interpreted to have formed at ~2650 to 2655 Ma (Fig. 5), with possibly earlier, noneconomic Mo ± Au mineralization associated with mafic and syenitic granites (e.g., Sunrise Dam, Granny Smith: Ojala, 1995; Brown et al., 2002).

Timmins-Val d'Or gold belt

The Timmins-Val d'Or gold belt (Fig. 10) is defined by the linear distribution of gold deposits along the Porcupine-Destor and Larder Lake-Cadillac fault zones and occupies an area of about 400 by 75 km in the southern part of the Abitibi subprovince (Fig. 1). Older volcanic cycles, formed between 2750 and 2710 Ma, are well represented in the area surrounding the Timmins-Val d'Or gold belt, where they comprise various proportions of mafic-ultramafic and intermediate to felsic volcanic rocks (Figs. 10, 11; Ayer et al., 2002). However, the 2710 to 2695 Ma volcanic rock sequence is much more restricted in distribution and overlaps very closely with the gold belt (Fig. 10). This sequence comprises a lower komatiitic unit, a middle tholeiitic, locally Fe-rich, basaltic unit, and an upper mafic to felsic rock unit of tholeiitic to calc-alkaline affinity, which were deposited, in part, on the older volcanic rock units (Ayer et al., 2002). Clastic sedimentary rocks are

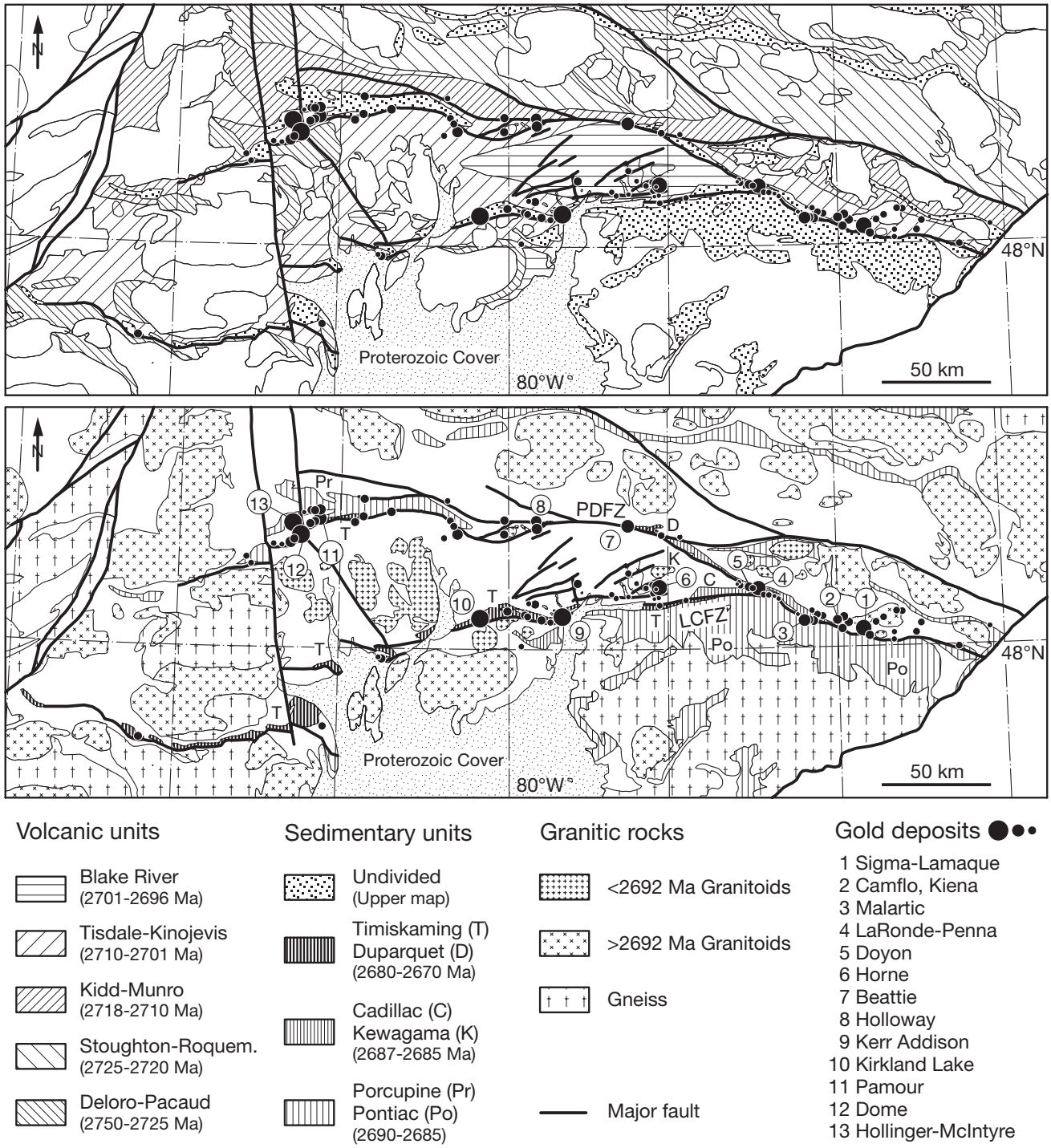

FIG. 10. Geologic map of the Timmins-Val d'Or gold belt. Compiled from MERQ-OGS (1983), Robert and Poulsen (1997), and Ayer et al. (2002). LCFZ = Larder Lake-Cadillac fault zone, PDFZ = Porcupine-Destor fault zone.

not voluminous in the Timmins-Val d'Or gold belt and occur mainly as narrow belts along the Porcupine-Destor and Larder Lake-Cadillac fault zones. Older sequences consist mainly of turbititic graywacke, with local conglomerate and BIF (Fig. 10), and were deposited between 2690 and 2685 Ma (Fig. 11; Davis, 2002; Ayer et al., 2003). The younger sedimentary rocks of the Timiskaming Group were deposited above angular unconformities between 2679 and 2670 Ma, mainly in fluvial to alluvial settings (Corfu et al., 1991; Ayer et al., 2003). These are locally accompanied by alkalic volcanism at ~2675 Ma.

Plutonism spans the same age range as volcanism and sedimentation but continued until about 2650 Ma (Fig. 11). Most of the pre-2700 Ma intrusions are sodic in composition and

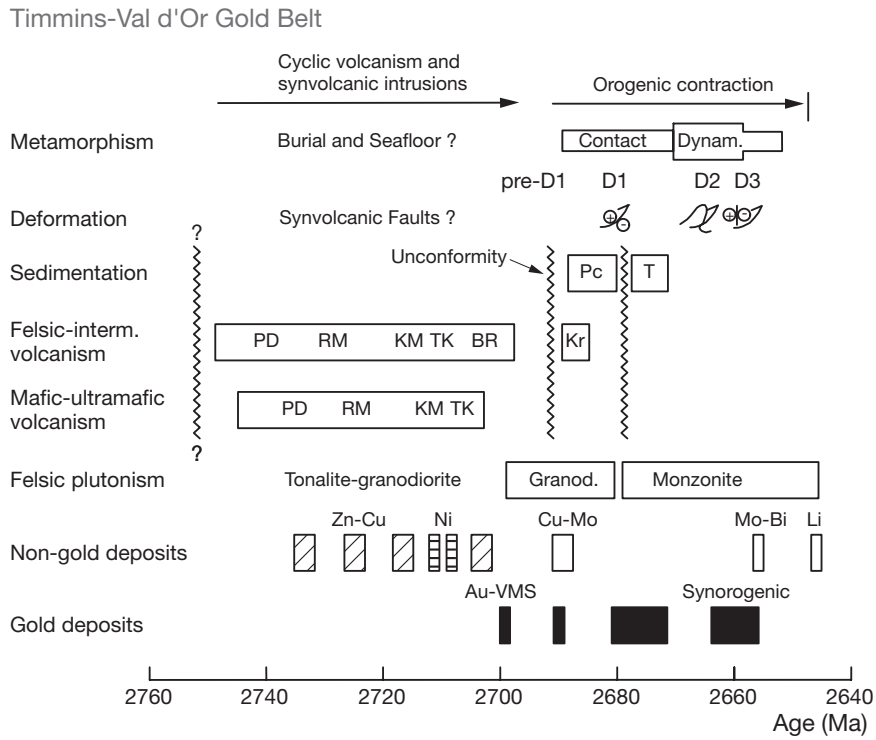

FIG. 11. Tectonic and metallogenic evolution diagram for the Timmins-Val d'Or gold belt. Data from Corfu (1993), Robert (2001), and Ayer et al. (2002, 2003). Abbreviation as in Figures 6C, 10.

dominated by tonalite and quartz diorite and are clearly synvolcanic (Sutcliffe et al., 1993; Rive et al., 1990). Postvolcanic pre-Timiskaming intrusions were emplaced between about 2692 and 2680 Ma and overlap in age with turbiditic sedimentation (Fig. 11). They range in composition from granodiorite to syenite and commonly occur in gold camps in the form of porphyry stocks and dikes. Younger syenitic rocks were also emplaced in the Kirkland Lake area between 2675 and 2670 Ma, synchronous with Timiskaming sedimentation. Post-Timiskaming felsic intrusions are rare in the gold belt and include the ~2645 Ma Lamotte and Lacorne monzogranite pluton (Ducharme et al., 1997).

All supracrustal rocks of the Timmins-Val d'Or gold belt are metamorphosed to assemblages of low- to medium-pressure, prehnite-pumpellyite to amphibolite facies (App. Fig. A8). With the exception of those in the prehnite-pumpellyite facies, metamorphic rocks contain penetrative metamorphic foliation and lineation (e.g., Jolly, 1974), particularly near major fault zones. Most geochronological data suggest that this regional dynamothermal metamorphism took place at ~2660 Ma (Powell et al., 1995a), although contact metamorphism adjacent to specific intrusions (e.g., Lamotte and Lacorne plutons) both pre- and postdated this regional metamorphism (Fig. 11).

Most rocks in the area have been heterogeneously strained to produce folds, foliations, and lineations that define an anastomosing but overall east-west structural trend (Fig. 10). Shortening in the area is a product of transpressive deformation involving north-south shortening and local strike-slip deformation (Hodgson and Hamilton, 1989; Daigneault et al., 2002). The resulting penetrative D_2 to D_3 foliation, lineation, and shape fabrics in strained rocks correspond to the ~2660 Ma regional metamorphism (Wilkinson et al. 1999; Fig. 11). Larger scale structural elements include major folds, Timiskaming and pre-Timiskaming angular unconformities, and inferred premetamorphic, major reverse faults (Powell et al., 1995b). The earlier pre-Timiskaming deformation is commonly assigned to a D_1 generation of structures (Fig. 11); locally, older pre-D_1 structures have also been documented in the Timmins district (Bleeker, 1995). Faults and shear zones of different orders impart a reticulate to anastomosed pattern of faulting in the Timmins-Val d'Or gold belt (Fig. 10). Most workers regard the kinematically complex first-order shear zones as steep thrusts, with minor dextral or sinistral movements resulting from their local strike-slip reactivation (Wilkinson et al., 1999). The existence of similar metamorphic pressures on opposite sides of the first-order faults precludes major postmetamorphic differential uplift on the faults (Powell et al., 1995a).

Numerous tectonic models have been proposed to explain the development of the Abitibi and adjacent subprovinces. During the last 30 years there has been a shift away from models requiring autochthonous development of the rocks in the Abitibi subprovince (Goodwin, 1977) toward those involving allochthonous terranes and generally invoking northward-dipping subduction, southward migration of trenches and arcs, and an ultimate collision involving terrane-scale thrusting (Dimroth et al., 1983; Hodgson and Hamilton, 1989; Wyman et al., 2002). However, autochtonous models have most recently been proposed again (Ayer et al., 2002), in

light of geochronological data for the mafic-ultramafic rock sequences, indicating similar geology across much of the southern Abitibi subprovince, albeit on juvenile crust.

Gold deposits in the Timmins-Val d'Or gold belt are mainly distributed along the Destor-Porcupine and Larder Lake-Cadillac fault zones (Fig. 10). Well-defined camps along these fault zones account for the majority of significant deposits and show a regular spacing of ~50 km. In addition, several styles of mineralization are represented among the large deposits, including the massive sulfide deposits at Horne and LaRonde-Penna, sulfide-rich vein deposit at Doyon, disseminated-stockwork deposits of felsic rock association at Malartic, and the dominant quartz-carbonate veins deposits at Hollinger-McIntyre, Dome, Kirkland Lake, and Sigma-Lamaque (Robert and Poulsen, 1997). Field and geochronological studies further indicate that these deposits also formed at different times in the evolution of the gold belt (Figs. 5, 11), with the formation of gold-rich massive sulfide deposits at the end of the main phase of volcanism at ~2696 Ma, syenite-associated disseminated-stockwork deposits near the time of Timiskaming sedimentation, and post-Timiskaming quartz-carbonate vein deposits synchronously with the late D_2 shortening between 2670 and 2660 Ma, but with some examples forming at ~2692 Ma as well (Fig. 11; Couture et al., 1994; Robert and Poulsen, 1997; Robert, 2001). Finally, this gold belt is also host to numerous zinc-copper VMS deposits, including the world-class Kidd Creek deposit and a few komatiite-associated nickel sulfide deposits (Card and Poulsen, 1998).

Rice Lake-Pickle Lake gold belt

The Rice Lake-Pickle Lake gold belt (Fig. 1) is defined by the alignment of a few isolated clusters of gold deposits that occupy a 50- by 450-km corridor that extends across the greenstone belts of the Uchi subprovince (Fig. 12). This subprovince is located between the North Caribou protocraton in the north, a Mesoarchean landmass overlain and overprinted by Neoarchean volcanic, sedimentary, and plutonic rocks, and the English River metasedimentary rock subprovince in the south (Fig. 1). Although the boundary between the Uchi and English River subprovinces is largely marked by the east-west Sydney Lake fault system (Stott and Corfu, 1991), gold deposits of the belt are not associated with this regional fault system but rather with less continuous and less well-defined fault zones (Fig. 12). The Rice Lake-Pickle Lake gold belt contains abundant Mesoarchean basalt and komatiite sequences, which are unconformably overlain by, and locally in fault contact with, Neoarchean mafic-felsic volcanic rock sequences (Stott and Corfu, 1991; Corfu et al., 1998). This stratigraphic succession is similar to that in the Red Lake Camp (Fig. 6D), except for the fact that the upper part of the Mesoarchean sequences includes, in places, felsic pyroclastic rocks that are capped by stromatolitic carbonate and BIF (Thurston and Chivers, 1990). Clastic sedimentary sequences with BIF are present in both the Mesoarchean and Neoarchean successions, and local unconformable sequences of sandstone and conglomerate, dated at <2705 Ma, represent the youngest supracrustal rocks in the gold belt (Figs. 12, 13).

This gold belt contains a wide range of ages and compositions of granitoid rocks (Fig. 13). Tonalitic rocks older than 3.0 Ga locally form the basement to Mesoarchean greenstone belts (Percival, 2003). Younger Mesoarchean granitoid rocks, intruded between 2870 and 2810 Ma, are present in the Rice Lake and Red Lake camps, but the bulk of granitoid rocks in

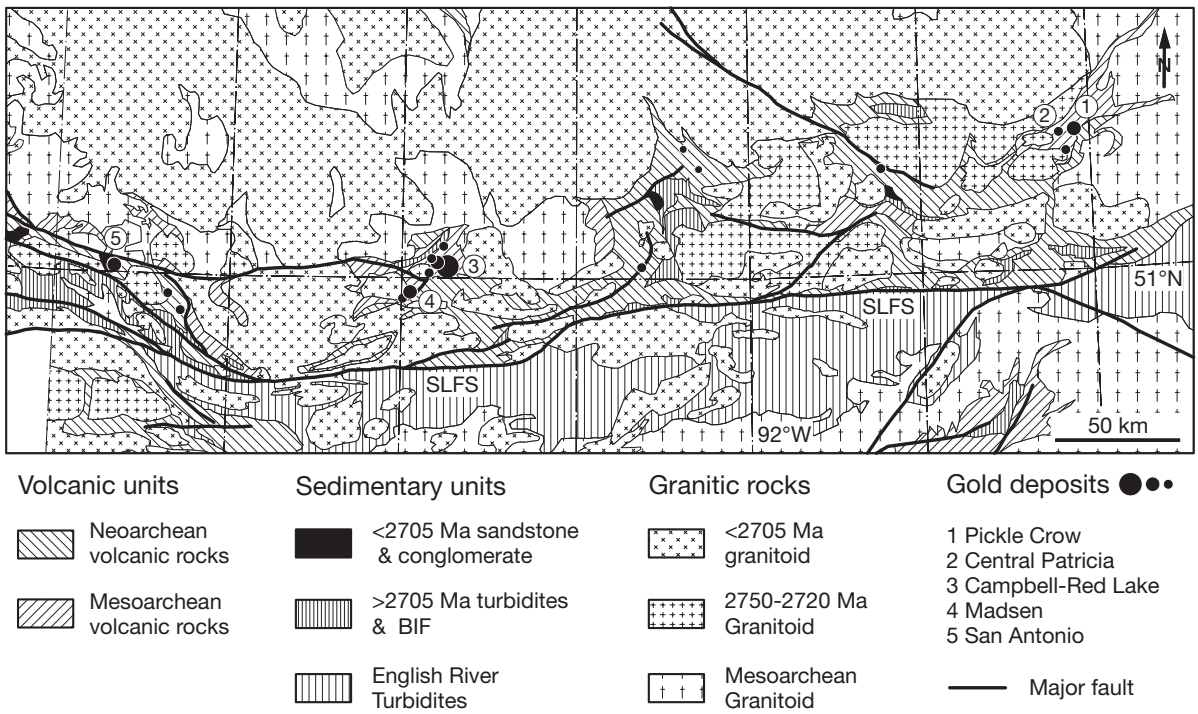

FIG. 12. Geologic map of the Rice Lake-Pickle Lake gold belt. Compiled from Thurston and Breaks (1978), Wallace et al. (1986), and Sanborn-Barrie et al. (2001). SLFS = Sydney Lake fault system.

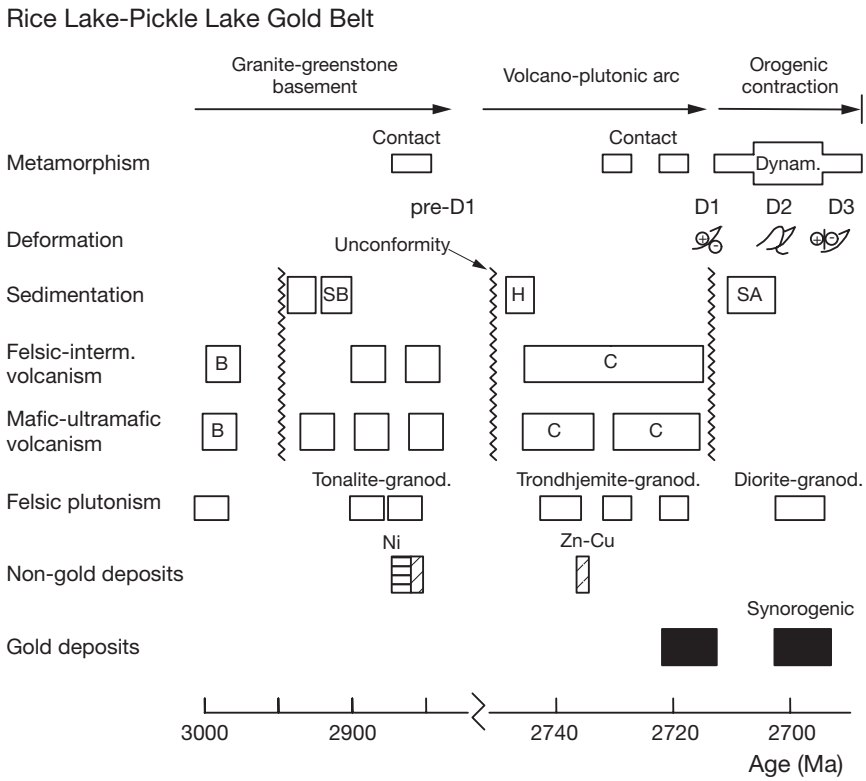

FIG. 13. Tectonic and metallogenic evolution diagram for the Rice Lake-Pickle Lake gold belt. Data from Corfu and Andrews (1987), Corfu and Davis (1992), Corfu and Stott (1993), Sanborn-Barrie et al (2001), and Dubé et al. (2004a). Abbreviations as in Figures 6D, 7D. SA = San Antonio Formation.

this belt are Neoarchean and and formed mainly in three intervals; from 2745 to 2740, 2730 to 2720, and 2702 to 2693 Ma (Fig. 13; Turek et al., 1989; Corfu and Stott, 1993). The first two suites are typically composed of tonalite and granodiorite and are coeval with volcanic rocks. The third suite, emplaced during the final stages of tectonism in the belt (Corfu and Stott, 1993), consists mainly of crustally contaminated diorite and granodiorite.

Metamorphic assemblages in the Rice Lake-Pickle Lake gold belt range from subgreenschist to upper amphibolite facies (App. Fig. A9). The amphibolite facies rocks tend to be developed in well-defined aureoles adjacent to Neoarchean granitoid batholiths and thus may be products of local contact metamorphism. Broad areas of greenschist and subgreenschist-grade rocks occur in the centers of greenstone belts and are distributed at intervals of approximately 100 km along the trend of the Rice Lake-Pickle Lake gold belt (Fig. A9). Much of the metamorphism in this belt is inferred to be coeval with the ~2702 to 2693 Ma granite magmatism and deformation (Corfu and Stott, 1993), although there is local evidence of earlier Mesoarchean deformation and metamorphism (Fig. 13; Percival, 2003).

A full understanding of the deformational history of the Rice Lake-Pickle Lake gold belt is complicated by the overprinting of Neoarchean structural events on Mesoarchean features. Angular unconformities at the base of Neoarchean volcanic rock sequences (Fig. 6D) provide evidence for early (pre-D_1) deformation. Most penetrative deformation (D_2) in the Uchi subprovince is arguably younger than ~2710 Ma, which is the approximate age of the youngest deformed volcanic and sedimentary units, although there are older structures in some localities as well (Stott and Corfu, 1991; Dubé et al., 2004a). The youngest structures in the belt are assigned to D_3 or younger (D_4) deformation and were responsible for dextral transcurrent displacement along the Sydney Lake fault system (Stott and Corfu, 1991).

Langford and Morin (1976) proposed that the Uchi subprovince represents an oceanic arc developed above a northerly dipping subduction zone, with the English River subprovince representing a forearc turbiditic basin or accretionary wedge. The Uchi arc was subsequently accreted to the North Caribou protocraton, comprising the Berens River and Sachigo subprovinces to the north (Fig. 1). More recent work continues to support such a model, with the recognition that at least part of the Neoarchean volcanic rocks of the Uchi subprovince developed directly on older continental crust (Sanborn-Barrie et al., 2001). Plume-related magmatism is also regarded as the likely cause of the Mesoarchean komatiites at Red Lake and Rice Lake (Hollings et al., 1999).

The gold camps along the Rice Lake-Pickle Lake gold belt occur in areas that preserve high proportions of volcanic rocks at relatively low metamorphic grade and show a regular spacing of 75 to 100 km (Figs. 12, A9). A majority of the gold camps also contain exposures of the rare <2704 Ma conglomerate-sandstone sequences known in the Uchi subprovince. Available data indicate that multiple ages of gold

mineralization must exist in this belt (Figs. 6, 13), including the possibility of some minor deposits having formed in the Mesoarchean (Gulson et al., 1993). Different styles of mineralization are also clearly present, with quartz-carbonate vein and sulfidic replacements of BIF most common along the belt but with crustiform vein-sulfidic replacement-style mineralization in the Campbell-Red Lake deposit representing by far the largest gold accumulation in the belt.

Comparison among gold belts

Although all four gold belts share similar volcanic, plutonic, deformation, and metamorphic histories, a number of geologic features combine to distinguish them from their surrounding greenstone areas and may be regarded as favorable indicators of well-endowed belts. The first is the presence of substantial volumes of ultramafic komatiites in the lower parts of the stratigraphic successions, rocks that are not uniformly present nor uniformly abundant in greenstone belts of the Superior and Yilgarn cratons. It is noteworthy that the two best-endowed belts, Timmins-Val d'Or and Wiluna-Norseman, contain the largest volumes of komatiites, with multiple ages in the former belt. A second aspect is the presence of some of the youngest supracrustal rock sequences present in their host province or subprovince. The Timmins-Val d'Or and Wiluna-Norseman gold belts, for example, contain the youngest volcanic rocks in their host cratons and the youngest, <2704 Ma, sandstone-conglomerate sequences of the Uchi subprovince are largely restricted to the area of the gold belt itself (Fig. 12). The third aspect is the presence of at least some areas of subgreenschist metamorphic-grade rocks somewhere along the belts, in some cases despite the presence of significant volumes of amphibolite-grade rocks, such as in the Rice Lake-Pickle Lake belt (Fig. A9). The last two features highlight a high degree of preservation of supracrustal sequences.

The gold belts also share the presence of multiple styles of large gold deposits, which are demonstrably of two or more distinct ages in three of the belts (Fig. 5), although such multiplicity of styles is also known in less well-endowed greenstone areas, such as in the Chibougamau area in the northeastern part of the Abitibi subprovince (Fig. 2; Guha et al., 1988). It is probably significant that the two most prolific gold belts also contain other world-class metal deposits: VMS deposits along the Timmins-Val d'Or gold belt and komatiite-associated nickel-sulfide deposits along the Wiluna-Norseman gold belt. Within the gold belts, the distribution of the camps is largely controlled by belt-scale fault zones, along which they commonly coincide with a change in the trend of the faults, with the exception of the Rice Lake-Pickle Lake belt. The camps further show a close spatial association with unconformities, as well as with structural highs that juxtapose the lower and uppermost parts of the stratigraphic columns.

Discussion

Historical perspective

The Archean gold deposits of the Superior and Yilgarn cratons were discussed in the *Economic Geology Fiftieth Anniversary Volume* in terms of metallogeny and structural geology. From a metallogenic point of view, Turneaure (1955) referred to gold deposits in the Kirkland Lake-Cadillac, Porcupine, and Western Australia metallogenic provinces as associated with Algoman granites and as having formed during the Algoman metallogenic epoch. He further noted the spatial association of the deposits with major fault zones, which were subjected to latest movements in the Algoman orogeny. He suggested a similarity of setting of the Kirkland Lake-Cadillac belt to that of younger terranes, such as those of the Sierra Nevada foothills in California. The deposits themselves were described to be of hypothermal to mesothermal character, in keeping with depth zoning models of the time. Of interest to the present discussion, the base metal-rich deposits in these provinces, including the Horne deposit, were considered to be of the same genetic style as the gold-bearing quartz veins and sulfidic replacements. In reviewing structural aspects of the Archean gold deposits, McKinstry (1955) also noted the importance of major fault zones in the Abitibi subprovince and in Western Australia and their similarities with the Mother Lode belt of deposits in California. He emphasized the importance of fluid channelways and recognized that the nature and orientations of fractures are controlled by external stresses coupled with the orientation and strength of host rocks. Drawing on examples from the Norseman and Val d'Or camps, McKinstry (1955) suggested that vein deposits are the result of both open-space filling and, as he termed it, "replacement" in shear and tension fractures and that, unlike in younger epithermal environments, reverse and strike-slip faults are dominant. He further described the deposits at Geraldton, Pickle Lake, and Southern Cross as concordant, "replaced" iron formations formed by secondary fracturing and veining.

The gold deposits and gold belts described herein received scant coverage in the *Economic Geology Seventy-Fifth Anniversary Volume*, perhaps reflecting the diminished economic importance of gold deposits in the preceding years. Nonetheless, a discussion of ore-forming processes related to gold-bearing quartz veins (Meyer, 1981) contained significantly different views than 25 yr earlier. The base metal-rich massive sulfide deposits by this point were accepted as being volcanogenic in origin and separated from the discussion. The gold-bearing quartz veins were portrayed as being of two styles. The majority, termed gash veins by Meyer (1981), were suggested to be the products of medium-temperature metamorphism accompanying deformation. In contrast, a few deposits were acknowledged to be metasomatic systems, generated at greater depth but with the view that the gold probably came from adjacent rocks (Meyer, 1981). The stratigraphic control of deposits and the notion of source beds were also emphasized at that time. The view was that the gold ores are effectively strata bound and localized high in the stratigraphic column. Looking at the problem from the view of Archean metallogeny, Anhaeusser (1981) expressed many of the same ideas, suggesting that gold was mobilized from a primary source and subsequently concentrated in a secondary setting. He noted that the relative abundance of gold in greenstone belts may be dictated by particular rock types, and that there is a close genetic tie between gold and ultramafic-mafic rock stratigraphy, particularly komatiites. In addition, he stated that gold orebodies are commonly associated with beds of sulfide and mixed sulfide-carbonate facies

BIF and regarded many such deposits as submarine chemical precipitates. From the perspective of timing, Anheusser (1981) suggested that the gold deposits, except for the "syngenetic-strata-bound occurrences," are epigenetic and generally produced by "relocation" in any favorable lithologic setting in the greenstone pile after granite emplacement, deformation, and metamorphism.

The last 25 yr coincided with a period of high economic interest for gold, which resulted in a considerable amount of research on Archean gold deposits, particularly in the Yilgarn and Superior cratons. The extensive geologic and geochronologic database developed in the last 25 yr indicates that similar tectonic processes took place in many, if not all, greenstone belts of the Superior and Yilgarn cratons. Although all greenstone belts contain at least some gold, only a few belts, and, more typically, very limited sectors within them, contain significant amounts, which points to the special character of such well-endowed areas. The most prolific sectors of greenstone belts are distinguished from their poorer counterparts mainly by a higher degree of preservation of supracrustal rocks and by more abundant komatiites. The composition of the substrate to the well-mineralized greenstone belts seems unimportant, with both ensialic and ensimatic environments represented. The distribution of large gold deposits and camps along narrow, continuous gold belts that commonly overlap with belt-scale fault zones is now understood to represent a spatial association with long-lived structures that acted as crustal scale magma and fluid conduits, which have also influenced coarse clastic sedimentation (Dimroth et al., 1982; Hallberg, 1986). However, the common regular spacing of large deposits or camps on the order of 30 to 50 km along fault zones is an empirical fact that remains mainly unexplained (Weinberg et al., 2004).

The intensive deposit-scale research of the last 25 yr has resulted in a better appreciation of local factors that control the location and geometry of the deposits. In addition to the reinforcement of the concept of the fundamental importance of faults and shear zones, these include the importance of competency contrast and layer anisotropy as factors influencing the orientation and degree of rock fracturing, a prime control on the location of mineralization, as well as the importance of rocks with a high Fe/(Fe + Mg) as a favorable chemical receptor for gold. The diverse styles of gold mineralization are now understood as having formed over a range of crustal depths, from epizonal to mesozonal, and possibly hypozonal (Groves, 1993; Goldfarb et al., 2005).

Issues of ages, models, and sites of gold deposits

Significant uncertainty and debate remain on the timing of formation of the deposits, the models that best explain their characteristics, and the fundamental causes of the high concentration of gold in very localized areas. The geologic and geochronologic evidence compiled in this review indicates clearly that the most gold deposits formed during the orogenic phase of the evolution of their host greenstone belts and can therefore be regarded as orogenic in a broad sense. However, given the evidence for multiple gold mineralizing events in each of the gold belts and for superposition of different ages of gold mineralization in a number of camps and deposits (Fig. 5), it is clear that no single mineralizing event can explain the formation of all gold deposits within the different gold belts.

Various models have been proposed to explain gold deposits in both cratons (e.g., Hodgson, 1993; Hutchinson, 1993; Spooner, 1993; Groves et al., 2003). The orogenic model, which relates diversity in styles of Au-only mineralization to depth variations during a single ore-forming period that occurs during the late, shortening stages of greenstone belt evolution (Groves et al., 2000) is clearly applicable to the abundant late-stage quartz-carbonate veins and other, temporally associated mineralization styles. Deposits that have been overprinted by late-stage deformation and metamorphism, or that possess unique Au base metal associations, require the application of other models (Groves et al., 2003). The Au-rich massive sulfide-style deposits of the Timmins-Val d'Or gold belt have been interpreted as transitional between classic VMS and shallow-marine epithermal deposits (Dubé et al., 2004b). Magmatic hydrothermal models have also been proposed for Au-only deposits (Spooner, 1993). More specifically, early-stage porphyry-type magmatic hydrothermal models have been applied to deposits such as the Au-Cu Boddington (Roth et al., 1991) and Troilus (Fraser, 1993) deposits, the Cu-Mo-Au McIntyre deposit (Davies and Lutha, 1978), and the Au-Mo Hemlo deposit (Muir, 2002). However, a late-stage (postorogenic) intrusion-related model has also been proposed for Boddington (McCuaig et al., 2001), as have syngenetic, epithermal, and orogenic models for Hemlo (Muir, 2002). Finally, epithermal models have also been proposed for the Campbell-Red Lake (Penzak and Mason, 1999) and Golden Mile (Clout, 1989) deposits.

Many of the divergent views on the genesis of gold deposits can be reconciled by considering a scenario of progressive formation of gold deposits in relationship to the different processes that take place along the gold belts during orogeny. In the right environment, the waning of volcanism and onset of uplift that result in voluminous clastic sedimentation may favor emergent felsic volcanism and the formation of shallow-marine Au-rich VMS deposits. The subsequent period of clastic sedimentation, early contractional deformation (D_1), and uplift that leads to development of various unconformities was accompanied by increased plutonic activity, including locally abundant shallow-level porphyry stocks and dikes. Magmatic hydrothermal deposits of porphyry affinity, or perhaps epithermal deposits, would be expected to form during this period. During the main phase of contractional deformation (D_2-D_3), burial and regional metamorphism, and the onset of the final unroofing of the greenstone belts, progressive and widespread formation of synorogenic deposits would be expected over a range of crustal depths. Such progressive formation of different types of gold deposits at different times along the same narrow belts could explain the common overprinting of the early deposit types by the late orogenic ones. By way of comparison, the diversity of styles of gold deposits formed during the 30- to 50-m.y. orogenic phase of the gold belts of both cratons rivals that of the Great Basin in western United States during the Cretaceous-Tertiary. That time period saw the formation of porphyry, skarn, Carlin-type, and a variety of epithermal gold deposits (Cline et al., 2005; Simmons et al., 2005), illustrating the diversity that can exist in large gold-producing regions.

Finally, the issue of the occurrence of large gold deposits in space is of greater practical importance than their timing or genesis. Decades of research on the Archean gold deposits of the Yilgarn and Superior cratons have led to many alternatives to explain their gold endowment. Magmatic and orogenic (both metamorphism and deformation) processes are those most commonly invoked (see Goldfarb et al., 2005, for more details). The specific histories of the gold belts, and the known constraints on timing of gold deposits, suggest that all of these processes may have led to the formation of one or more specific deposits, and that it is virtually impossible to separate orogenic and magmatic processes because they overlap so completely in space and time. In addition, the products of volcanism, plutonism, metamorphism, and deformation are found in every greenstone belt, yet significant gold deposits are not. Mantle plumes have also been invoked to explain the gold endowment of the two cratons (Barley et al., 1998; Wyman et al., 1999). Although mantle plumes may be responsible for the formation of komatiites in all of the gold belts considered here, the fact that they significantly predate gold deposition, for example by as much as 300 m.y. in the Rice Lake-Pickle Lake gold belt, precludes their direct bearing on the origin of gold deposits.

The linear arrangement of deposits in gold belts is commonly attributed to crustal-scale faults. Late tectonic faults and shear zones are commonplace in the Archean gold belts but not all of them share the same ancestry or the same gold endowment. Considerable emphasis has been placed on the kinematics of such structures, as deduced by their late-stage metamorphic fabrics, but a more important issue is their earlier history as loci of magmatism and coarse clastic sedimentation (e.g., Dimroth et al., 1982; Hallberg, 1986). The best-endowed gold belts appear to be those associated with long-lived crustal structures that have influenced the early, precontractional deformation and geological development of the belts, including voluminous komatiitic volcanism and basin architecture, as well as the presence, and high degree of preservation, of young supracrustal rocks. Although synorogenic quartz-carbonate vein and BIF-hosted gold occurrences are present throughout the greenstone belts of both cratons, large examples of such deposits are mainly restricted to gold belts. These belts are also marked by the presence of large examples of other, commonly atypical, deposit styles, which perhaps represents another key signature of the well-endowed belts. Again, by comparison, the concentration of significant gold deposits in well-defined gold belts is not a unique feature of the Superior and Yilgarn cratons. For example, in the Great Basin, gold deposits are also arranged in specific gold belts containing more than one age and style of deposit, such as in the Walker Lane, the Battle Mountain-Eureka trend, and the Carlin trend (Cline et al., 2005). This must be a reflection of fundamental crustal structure, and perhaps composition of subcrustal mantle, as much as the local ore-forming hydrothermal processes (Hildenbrand et al., 2000).

Outstanding issues for future research

It is clear from this review that we are still lacking an in-depth geologic understanding (in the broad sense) of many world-class gold deposits and the fundamental controls on their distribution at the camp and belt scales in the Superior and Yilgarn cratons. As pointed out by Groves et al. (2003), progress on this critical front will require careful integration of thorough field-based studies with more sophisticated geochemical and isotopic studies. It will be critical that the work emphasizes the types of geologic, stratigraphic, and structural relationships that have been highlighted here at the deposit, camp, and belt scales. It will be just as critical that such work be carried out by integrated research teams.

Future research into the gold metallogeny of Archean cratons should focus on the following particularly critical topics: (1) detailed and integrated documentation of large gold deposits is needed, particularly for those that remain enigmatic, including their absolute and relative timing with respect to other geologic events, and their camp-scale settings, in order to highlight the key geologic controls of their location and development; (2) the early geologic history of the prolific gold belts, the possible special aspects of the associated long-lived crustal-scale structures, and the causes of regular spacing of camps along them, all need to be deciphered; (3) the relationships of gold deposits to metamorphism need to be clarified, particularly in areas of high metamorphic grade—this also calls for a better understanding of the thermal histories of the greenstone belts; and (4) the causes of the heterogeneous gold endowment within the cratons and the greenstone belts, which may be related to the ultimate source of gold within them, need consideration.

Conclusions

The foregoing review of the temporal and spatial controls on gold deposits and camps of the Yilgarn and Superior cratons suggests several broad conclusions. Significant gold deposits are concentrated in narrow, continuous gold belts (Timmins-Val d'Or and Wiluna-Norseman), each accounting for >50 percent of the gold endowment of their respective cratons. The linear arrangement of deposits in these gold belts is commonly attributed to crustal-scale faults (e.g., Boulder-Lefroy, Destor-Porcupine). Considerable emphasis has been placed on the kinematics of such structures, as deduced by their late-stage metamorphic fabrics, but a more important issue is their earlier history as loci of magmatism and coarse clastic sedimentation. Gold deposits, including large ones, cluster into camps, spaced about 30 to 50 km along the belts and commonly sited at bends in the trace of controlling crustal scale faults. The most prolific gold camps are characterized by structural highs that juxtapose the lower and uppermost parts of the stratigraphic column and by folded unconformities, early regional alteration, and concentrations of intermediate to felsic porphyry stocks.

The great gold belts contain significant volumes of komatiites, and the upper parts of Archean crust are well preserved. The belts contain rocks metamorphosed to subgreenschist facies and some of the youngest volcanic and clastic sedimentary rocks that occur in their respective cratons. The nature of the subvolcanic crust seems to be unimportant in determining the prospectivity of a gold belt. Extensive komatiitic volcanism, polycyclic in the case of the Abitibi subprovince, is perhaps the first tangible reflection of a connection to the deep crust and mantle, even if not directly related in time to mineralization. Unconformities, irrespective of the age and

composition of the rocks above them, are commonly loci for many deposits and camps within the belts. Although there are many possible explanations for this association, they most likely are expressions at the Archean surface of the structures that ultimately control the locations of deposits.

There is no single event that explains the formation of all gold deposits in either craton. Rather, gold belts, camps, and even some deposits contain different styles of ore, clearly formed at different times and, in many cases, by different processes. Despite the diachroneity of gold deposition, the majority of deposits formed toward the end of the tectonic histories of their respective cratons. Most deposits, irrespective of genesis, formed between 2720 and 2630 Ma, an interval of time approximately equivalent to the latest Cretaceous through Tertiary.

Decades of research on the Archean gold deposits of the Yilgarn and Superior cratons have led to many alternatives to explain the gold endowment of these cratons, most commonly invoking magmatic and orogenic (metamorphism and deformation) processes. The specific histories of the gold belts, and the known constraints on timing of gold deposits, suggest that all of these processes may have led to the formation of one or more specific deposits and that it is virtually impossible to separate orogenic and magmatic processes because they overlap so completely in space and time. The only constant is one of place, such that the products of volcanism, plutonism, metamorphism, and deformation are found in every greenstone belt, yet significant gold deposits are not. Irrespective of a century of debate on ore genesis, a unique explanation for the exceptional gold endowment of specific belts and camps remains elusive.

Acknowledgments

The information and ideas presented in this review rely on the research of many people and far more references than can be acknowledged within the space allocated. Where appropriate, original key papers have been cited, but recent review-type papers, themselves containing extensive additional references, have also been cited widely. The authors wish to acknowledge B. Dubé, R.J. Goldfarb, D.I. Groves, and T.C. McCuaig, whose constructive comments greatly improved the quality of the paper, as well as many colleagues for important discussions on gold deposits in the Yilgarn and Superior cratons. FR and CJH thank Barrick Gold Corporation, and KFC, the Chief Executive Officer of Geoscience Australia, for permission to publish.

REFERENCES

Agterberg, F.P., 1995, Multifractal modeling of the sizes and grades of giant and supergiant deposits: International Geology Review, v. 37, p. 1–8.

Andrews, A.J., Hugon, H., Durocher, M., Corfu, F., and Lavigne, M.J., 1986, The anatomy of a gold-bearing greenstone belt: Red Lake, northwestern Ontario, Canada, *in* Macdonald, A.J., ed., Gold '86: Willowdale, Ontario, Konsult International Inc., p. 3–22.

Anhaeusser, C.R., 1981, The relationship of mineral deposits to early crustal evolution: Economic Geology 75th Anniversary Volume, p. 42–62.

Ayer, J., Amelin, Y., Corfu, F., Kamo, S., Ketchum, J., Kwok, K., and Trowell, N.F., 2002, Evolution of the southern Abitibi greenstone belt based on U-Pb geochronology: Autochthonous volcanic construction followed by plutonism, regional deformation and sedimentation: Precambrian Research, v. 115, p. 63–95.

Ayer, J., Barr, E., Bleeker, W., Creaser, R.A., Hall., G., Ketchum, J.W.F., Powers, D., Salier, B., Still, A., and Trowell, N.F., 2003, Discover Abitibi. New geochronological results from the Timmins area: Implications for the timing of late tectonic stratigraphy, magmatism, and gold mineralization: Ontario Geological Survey Open File Report 6120, p. 33–1 to 33–11.

Baggott, M.S., Vielreicher, N.M., Groves, D.I., McNaughton, N.J., and Gebre-Mariam, M., in press, Evidence for post ca 2.66 Ga Archean lode-gold mineralization in the Yandal belt, Western Australia, from the high level, brittle-style Jundee-Nimary gold deposits: Economic Geology.

Barley, M.E., Eisenlohr, B.N., Groves D.I., Perring, C.S., and Vearncombe, J.R., 1989, Late Archean convergent margin tectonics and gold mineralization: A new look at the Norseman-Wiluna belt: Geology, v. 17, p. 826–829.

Barley, M.E., Krapez, B., Groves, D.I., and Kerrich, R., 1998, The late-Archean bonanza: Metallogenic and environmental consequences of the interaction between mantle plumes, lithospheric tectonics and global cyclicity: Precambrian Research, v. 91, p. 65–90.

Bateman, R., and Hagemann, 2004, Gold mineralization throughout about 45 Ma of Archean orogenesis: Protracted flux of gold in the Golden Mile, Yilgarn craton, Western Australia: Mineralium Deposita, v. 39, p. 536–559.

Binns, R.A., Gunthorpe, R.J., and Groves, D.I., 1976, Metamorphic patterns and development of greenstone belts in eastern Yilgarn block, Western Australia: New York, Wiley, p. 303–313.

Bleeker, W., 1995, Geology and ore deposits of the Porcupine mining camp: Geological Survey of Canada Open File Report 3141, p. 13–37.

Blewett, R.S., Cassidy, K.F., Champion, D.C., Henson, P.A., Goleby, B.R., Jones, L., and Groenewald, P.B., 2004, The Wangkathaa orogeny: An example of episodic regional "D2" in the late Archaean Eastern Goldfields province, Western Australia: Precambrian Research, v. 130, p. 139–159.

Böhkle, J.K., 1989, Comparison of metasomatic reactions between a common CO2-rich vein fluid and diverse wall rocks: Intensive variables, mass transfers, and Au mineralization, Alleghany, California: Economic Geology, v. 84, p. 291–327.

Boulter, C.A., Fotios, M.G., and Phillips, G.N., 1987, The Golden Mile, Kalgoorlie: A giant gold deposit localized in ductile shear zones by structurally induced infiltration of an auriferous metamorphic fluid: Economic Geology, v. 82, p. 1661–1678.

Brown, S.J.A., Krapez, B., Beresford, S.W., Cassidy, K.F., Champion, D.C., Barley, M.E., and Cas, R.A.F., 2001, Archaean volcanic and sedimentary environments of the Eastern Goldfields province, Western Australia—a field guide: Western Australia Geological Survey Record 2001/13, 66 p.

Brown, S.M., Fletcher, I.R., Stein, H.J., Snee, L.W. and Groves, D.I., 2002, Geochronological constraints on pre-, syn- and postmineralization events at the world-class Cleo gold deposit, Eastern Goldfields province, Western Australia; Economic Geology, v. 97, p. 541–559.

Bucci, L.A., McNaughton, N.J., Fletcher, I.R., Groves, D.I., Kositcin, N., Stein, H.J., and Hagemann, S.G., 2004, Timing and duration of high-temperature gold mineralization and spatially granitoid magmatism at Chalice, Yilgarn craton, Western Australia: Economic Geology, v. 99, p. 1123–1144.

Campbell, I.H., and Hill, R.I., 1988, A two stage model for the formation of granite-greenstone terrains of the Kalgoorlie-Norseman area, Western Australia: Earth and Planetary Science Letters, v. 90, p. 971–986.

Card, K.D., 1990, A review of the Superior province of the Canadian Shield, a product of Archean accretion: Precambrian Research, v. 48, p. 99–156.

Card, K.D., and Poulsen, K.H., 1998, Geology and mineral deposits of the Superior province of the Canadian Shield: Geological Survey of Canada, Geology of Canada, no. 7, p. 13–194.

Cassidy, K.F., and Champion, D.C., 2004, Crustal evolution of the Yilgarn craton from Nd isotopes and granite geochronology: Implications for metallogeny [ext. abs.]: Centre for Global Metallogeny, University of Western Australia Publication 33, p. 317–320.

Cassidy, K.F., Groves, D.I., and McNaughton, N.J., 1998, Late-Archean granitoid-hosted lode-gold deposits, Yilgarn craton, Western Australia: Deposit characteristics, crustal architecture, and implications for ore genesis: Ore Geology Reviews, v. 13, p. 65–102.

Cassidy, K.F., Champion, D.C., McNaughton, N.J., Fletcher, I.R., Whitaker, A.J., Bastrakova, I.V., and Budd, A.R., 2002, Characterisation and metallogenic significance of Archaean granitoids of the Yilgarn craton, Western Australia: Minerals and Energy Research Institute of Western Australia (MERIWA) Report 222, 514 p.

Champion, D.C., and Cassidy, K.F., 2002, Granites in the Leonora-Laverton transect area, northeast Yilgarn craton: Geoscience Australia Record 2002/18, p. 13–30.

Champion, D.C., and Sheraton, J.W., 1997, Geochemistry and Sm-Nd isotope systematics of Archean granites of the Eastern Goldfields, Yilgarn craton, Australia: Constraints on crustal growth: Precambrian Research, v. 83, p. 109–132.

Clark M.E., Carmichael, D.M., Hodgson, C.J., and Fu, M., 1989, Wall-rock alteration, Victory gold mine, Kambalda, Western Australia: Processes and P-T-X_{CO_2} conditions of metasomatism: Economic Geology Monograph 6, p. 445–459.

Cline, J.S., Hofstra, A.H., Muntean, J.L., Tosdal, R.M., and Hickey, K.A., 2005, Carlin-type gold deposits in Nevada: Critical geologic characteristics and viable models: Economic Geology 100th Anniversary Volume, p. 451–484.

Clout, J.M.F., 1989, Structural and isotopic studies of the Golden Mile gold-telluride deposit, Kalgoorlie, WA: Unpublished Ph.D. thesis, Clayton, Victoria, Australia, Monash University, 352 p.

Clout, J.M.F., Cleghorn, J.H., and Eaton, P.C., 1990, Geology of the Kalgoorlie goldfield, *in* Hughes, F.E., ed., Geology of the mineral deposits of Australia and Papua New Guinea: Australasian Institute of Mining and Metallurgy, p. 411–431.

Colvine A.C., 1989, An empirical model for the formation of Archean gold deposits: Products of final cratonization of the Superior province, Canada: Economic Geology Monograph 6, p. 37–53.

Corfu, F., 1993, The evolution of the southern Abitibi greenstone belt in light of precise U-Pb geochronology: Economic Geology, v. 88, p. 1323–1340.

Corfu, F., and Andrews, A.J., 1987, Geochronological constraints on the timing of magmatism, deformation, and gold mineralization in the Red Lake greenstone belt, northwestern Ontario: Canadian Journal of Earth Sciences, v. 24, p. 1302–1320.

Corfu, F., and Davis, D.W., 1992, A U-Pb geochronological framework for the western Superior province, Ontario: Ontario Geological Survey Special Volume 4, pt. 2, p. 1335–1346.

Corfu, F., and Stott, G.M., 1993, U-Pb geochronology of the central Uchi subprovince, Superior province: Canadian Journal of Earth Sciences, v. 30, p. 1179–1196.

Corfu, F., Jackson, S.L., and Sutcliffe, R.H., 1991, U-Pb ages and tectonic significance of late Archean alkalic magmatism and non-marine sedimentation: Timiskaming Group, southern Abitibi belt, Ontario: Canadian Journal of Earth Sciences, v. 28, p. 489–503.

Corfu, F., Davis, D.W., Stone, D. and Moore, M.L., 1998, Chronostratigraphic constraints on the genesis of Archean greenstone belts, northwestern Superior province, Ontario, Canada: Precambrian Research, v. 92, p. 277–295.

Couture J.F., Pilote P., Machado N., and Desrochers, J.P., 1994, Timing of gold mineralization in the Val d'Or district, southern Abitibi belt: Evidence for two distinct mineralizing events: Economic Geology, v. 89, p. 1542–1551.

Daigneault, R., Mueller, W.U., and Chown, E.H., 2002, Oblique Archean subduction: Accretion and exhumation of an oceanic arc during dextral transpression, Southern volcanic zone, Abitibi subprovince, Canada: Precambrian Research, v. 115, p. 261–290.

Davies, J.F., and Lutha, L.E., 1978, An Archean "porphyry-type" disseminated copper deposit, Timmins, Ontario: Economic Geology, v. 73, p. 383–396.

Davis, D.W., 2002, U-Pb geochronology of Archean metasedimentary rocks in the Pontiac and Abitibi subprovinces, Quebec: Constraints on timing, provenance and regional tectonics: Precambrian Research, v. 115, p. 97–118.

Davis, B.K., in press, Complexity of structure and mineralization history in the Eastern Goldfields province, Yilgarn craton: Economic Geology.

Davis, D.W., and Lin, S., 2003, Unraveling the geologic history of the Hemlo Archean gold deposit, Superior province, Canada: A U-Pb geochronological study: Economic Geology, v. 98, p. 51–67.

Dimroth, E., Imreh, L., Rocheleau, M., and Goulet, N., 1982, Evolution of the south-central part of the Archean Abitibi belt, Quebec. Part I. Stratigraphy and paleogeographic model: Canadian Journal of Earth Sciences, v. 19, p. 1729–1758.

Dimroth, E., Imreh, L., Goulet, N., and Rocheleau, M., 1983, Evolution of the south-central segment of the Archean Abitibi belt, Quebec. Part III. Plutonic and metamorphic evolution and geotectonic model: Canadian Journal of Earth Sciences, v. 20, p. 1374–1388.

Dubé, B., Williamson, K., and Malo, M., 2003, Gold mineralization within the Red Lake mine trend: Example from the Cochenour-Willans mine area, Red Lake, Ontario, with new key information from the Red Lake mine and potential analogy with the Timmins camp: Geological Survey of Canada Current Research 2003–C21, 21 p.

Dubé, B., Williamson, K., McNicoll, V.M., Malo, M., Skulski, T., Twomey, T., and Sanborne-Barrie, M., 2004a, Timing of gold mineralization at Red Lake, Northwestern Ontario, Canada: New constraints from U-Pb geochronology at the Goldcorp High-grade zone, Red Lake mine, and the Madsen mine: Economic Geology, v. 99, p. 1611–1641.

Dubé, B., Mercier-Langevin, P., Hannington, M.D., Davis, D.W., and Lafrance, B., 2004b, Le gisement de sulfures massifs volcanogènes aurifères LaRonde, Abitibi, Québec: altération, minéralisation, genèse et implications pour l'exploration: Ministère des Ressources Naturelles, Faune et Parcs, Québec MB 2004–03, 112 p.

Ducharme, Y., Stevenson, R.K., and Machado, N., 1997, Sm-Nd geochemistry and U-Pb geochronology of the Preissac and Lamotte leucogranites, Abitibi subprovince: Canadian Journal of Earth Sciences, v. 34, p. 1059–1071.

Emmons, W.H., 1937, Gold deposits of the world: New York, McGraw-Hill, 562 p.

Fletcher, I.R., Dunphy, J.M., Cassidy, K.F., and Champion, D.C., 2001, Compilation of SHRIMP U-Pb geochronological data, Yilgarn craton, Western Australia, 2000–2001: Geoscience Australia Record 2001/47, 111 p.

Franklin, J.M., Gibson, H.L., Jonasson, I.R., and Galley, A.G., 2005, Volcanogenic massive sulfide deposits: Economic Geology 100th Anniversary Volume, p. 523–560.

Fraser, R.J., 1993, The Lac Troilus copper-gold deposit, northwestern Quebec: A possible Archean porphyry system: Economic Geology, v. 88, p. 1685–1699.

Gaboury, D., and Daigneault, R., 1999, Evolution from sea floor-related to sulfide-rich quartz vein-type gold mineralization during deep submarine volcanic construction: The Géant Dormant gold mine, Archean Abitibi belt: Economic Geology, v. 94, p. 3–22.

Gauthier, L., Hagemann, S., Robert, F., and Pickens, G., 2004, New constraints on the architecture and timing of the giant Golden mile deposit, Kalgoorlie, Western Australia [ext. abs.]: Centre for Global Metallogeny, University of Australia Publication 33, p. 353–356.

Gebre-Mariam, M., Hagemann, S.G., and Groves, D.I., 1995, A classification scheme for epigenetic Archean lode-gold deposits: Mineralium Deposita, v. 30, p. 408–410.

Goldfarb, R.J., Groves, D.I., and Gardoll, S., 2001, Orogenic gold and geologic time: A global synthesis: Ore Geology Reviews, v. 18, p. 1–75.

Goldfarb, R.J., Baker, T., Dubé, B., Groves, D.I., Hart, C.J.R., and Gosselin, P., 2005, Distribution, character, and genesis of gold deposirts in metamorphic terranes: Economic Geology 100th Anniversary Volume, p. 407–450.

Goodwin, A.M., 1977, Archean basin-craton complexes and the growth of Precambrian Shields: Canadian Journal of Earth Sciences, v. 14, p. 2737–2759.

Gosselin, P., and Dubé, B., 2005, Gold deposits of the world: Distribution, geological parameters, and gold content: Geological Survey of Canada Open File 4895, 1 CD-ROM.

Gray, M.D., and Hutchinson, R.W., 2001, New evidence for multiple periods of gold emplacement in the Porcupine Mining District, Timmins Area, Ontario, Canada: Economic Geology, v. 96, p. 453–476.

Groves, D.I., 1993, The crustal continuum model for late-Archean lode gold deposits of the Yilgarn block, Western Australia: Mineralium Deposita, v. 28, p. 366–374.

Groves, D.I., and Batt, W.D., 1984, Spatial and temporal variations of Archean metallogenic associations in terms of evolution of granite-greenstone terrains with special emphasis on the Western Australian Shield, *in* Kroner, A., Hanson, G.N., and Goodwin, A.M., eds., Archean geochemistry: Berlin, Springer, p. 73–98.

Groves, D.I., and Phillips, G.N., 1987, The genesis and tectonic controls on Archean lode gold deposits of the Western Australian shield: A metamorphic-replacement model: Ore Geology Reviews, v. 2, p. 287–322.

Groves, D.I., Knox-Robinson, C.M., Ho, S.E., and Rock, N.M.S., 1990, An overview of Archean lode gold deposits: Geology Department and University Extension, University of Western Australia Publication 20, p. 2–18.

Groves, D.I., Ridley, J.R., Bloem, E.M.J., Gebre-Mariam, M., Hagemann, S.G., Hronsky, J.M.A., Knight, J.T., McNaughton, N.J., Ojala, J., Vielreicher, R.M., McCuaig, T.C., and Holyland, P.W., 1995, Lode gold deposits of the Yilgarn block: Products of late-Archean crustal-scale overpressured hydrothermal systems: Geological Society of London Special Publication 95, p. 155–172.

Groves, D.I., Goldfarb, R.J., Gebre-Mariam, M., Hagemann, S.G., and Robert, F., 1998, Orogenic gold deposits: A proposed classification in the context of their crustal distribution and relationships to other gold deposit types: Ore Geology Reviews, v. 13, p. 7–27.

Groves, D.I., Goldfarb, R.J., Knox-Robinson, C.M., Ojala, J., Gardoll, S., Yun, G.Y., and Holyland, P., 2000, Late-kinematic timing of orogenic gold deposits and significance for computer-based exploration techniques with emphasis on the Yilgarn block, Western Australia: Ore Geology Reviews, v. 17, p. 1–38.

Groves, D.I., Goldfarb, R.J., Robert, F., and Hart, C.J.R., 2003, Gold deposits in metamorphic belts: Overview of current understanding, outstanding problems, future research, and exploration significance: Economic Geology, v. 98, p. 1–29.

GSWA, 2005, East Yilgarn, 1:100,000 Geological Information Series (June 2005 update): Geological Survey of Western Australia.

Guha, J., Dubé, B., Pilote, P., Chown, E.H., Archambault, G., and Bouchard, G., 1988, Gold mineralization patterns in relation to the lithologic and tectonic evolution of the Chibougamau mining district, Quebec, Canada: Mineralium Deposita, v. 23, p. 298–298.

Gulson, B.L., Mizon, K.J., and Atkinson, B., 1993, Source and timing of gold and other mineralization in the Red Lake area, Northwestern Ontario, Canada, based on lead-isotope investigations: Canadian Journal of Earth Sciences, v. 30, p. 2366–2379.

Hagemann, S.G., and Cassidy, K.F., 2000, Archean orogenic gold deposits: Reviews in Economic Geology, v. 13, p. 9–68.

Hagemann, S.G., Groves, D.I, Ridley, J.R., and Vearncombe, J.R., 1992, The Archean lode gold deposits at Wiluna, Western Australia: High-level brittle-style mineralization in a strike-slip regime: Economic Geology, v. 87, p. 1022–1053.

Hall, D., Maclean, D., and Gebre-Mariam, M., 2003, The discovery of the Westside gold deposit, Jundee-Nimary goldfield, Western Australia: Case Histories of Discovery, NewGenGold 2003 Conference, Perth, 24–25 November 2003, Proceedings, p. 18–34.

Hall, R.S., and Rigg, D.M., 1986, Geology of the West anticline zone, Musselwhite prospect, Opapimiskam Lake, Ontario, Canada, *in* Macdonald, A.J., ed., Gold '86: Willowdale, Ontario, Konsult International Inc., p. 124–136.

Hallberg, J.A., 1985, Geology and mineral deposits of the Leonora-Laverton area, northeastern Yilgarn block, Western Australia: Perth, Western Australia, Hesperian Press, 140 p.

——1986, Archean basin development and crustal extension in the northeastern Yilgarn block, Western Australia: Precambrian Research, v. 31, p. 133–156.

Hildenbrand, T.G., Berger, B., Jachens, R.C., and Ludington, S., 2000, Regional crustal structures and their relationship to the distribution of ore deposits in the western United States based on magnetic and gravity data: Economic Geology, v. 95, p. 1583–1605.

Hodgson, C.J., 1993, Mesothermal lode-gold deposits: Geological Association of Canada Special Paper 40, p. 635–678.

Hodgson, C.J., and Hamilton, J.V., 1989, Gold mineralization in the Abitibi greenstone belt: End-stage results of Archean collisional tectonics?: Economic Geology Monograph 6, p. 86–100.

Hodgson, C.J., and MacGeehan, P.J., 1982, A review of the geological characteristics of "gold-only" deposits in the Superior province of the Canadian Shield: Canadian Institute of Mining and Metallurgy Special Volume 24, p. 211–229.

Hodgson, C. Jay, Hamilton, J.V., and Piroshco, D. W., 1990, Structural setting of gold deposits and the tectonic evolution of the Timmins-Kirkland Lake area, southwestern Abitibi greenstone belt, *in* Ho, S.E., Robert, F., and Groves, D.I., eds, Gold and base metal mineralization in the Abitibi subprovince, Canada, with emphasis on the Quebec segment: Geology Department (Key Centre) and University Extension, University of Western Australia, p. 101–120.

Hollings, P., Wyman, D., and Kerrich, R., 1999, Komatiite-basalt-rhyolite volcanic associations in northern Superior province greenstone belts: Significant of plume-arc interaction in the generation of the proto-continental Superior province: Lithos, v. 46, p. 137–161.

Huleatt, M.B., and Jacques, A.L., 2005, Australian gold exploration 1976–2003: Resources Policy, v. 30, p. 29–37.

Hutchinson, R.W., 1993, A multi-stage, multi-process genetic hypothesis for greenstone-hosted gold lodes: Ore Geology Reviews, v. 8, p. 349–382.

Hutchinson, R.W., Ridler, R.H., and Suffel, G.G., 1971, Metallogenic relationships in the Abitibi belt, Canada: A model for Archean metallogeny: Canadian Institute of Mining and Metallurgy Bulletin, v. 64, p. 48–57.

Jolly, W.T., 1974, Regional metamorphic zonation as an aid in the study of Archean terrain: Abitibi region, Ontario: Canadian Mineralogist, v.12, p. 499–508.

Keats, W., 1987, Regional geology of the Kalgoorlie-Boulder gold-mining district: Geological Survey of Western Australia Report 21, 44 p.

Kent, A.J.R., and McDougall, I., 1995, ^{40}Ar-^{39}Ar and U-Pb age constraints on the timing of gold mineralization in the Kalgoorlie gold ield, Western Australia: Economic Geology, v. 90, p. 845–859.

Kent, A.J.R., Cassidy, K.F., and Fanning, C.M., 1996, Archean gold mineralization synchronous with the final stages of cratonization, Yilgarn craton: Geology, v. 24, p. 879–882.

Kerrich, R., and Cassidy, K.F., 1994, Temporal relationships of lode gold mineralization to accretion, magmatism, metamorphism and deformation—Archean to present: A review: Ore Geology Reviews, v. 9, p. 263–310.

Krapez, B., Brown, S.J.A., Hand, J., Barley, M.E., and Cas, R.A.F., 2000, Age constraints on recycled crustal and supracrustal sources of Archaean metasedimentary sequences, Eastern Goldfields province, Western Australia: Evidence from SHRIMP zircon dating: Tectonophysics, v. 322, p. 89–133.

Langford, F.F., and Morin, J.A., 1976, The development of Superior province of northwestern Ontario by merging island arcs: American Journal of Science, v. 276, p. 1023–1034.

Lin, S., 2001, Stratigraphic and structural setting of the Hemlo gold deposit, Ontario, Canada: Economic Geology, v. 96, p. 477–507.

Lindgren, W., 1933, Mineral deposits: New York and London, McGraw-Hill, 930 p.

MacGeehan, P.J., and Hodgson, C.J., 1982, Environments of gold mineralization in the Campbell Red Lake and Dickenson mines, Red Lake district, Ontario: Canadian Institute of Mining and Metallurgy Special Volume 24, p. 184–210.

Marmont S., and Corfu F., 1989, Timing of gold introduction in the Late Archean tectonic framework of the Canadian Shield: Evidence from U-Pb zircon geochronology of the Abitibi subprovince: Economic Geology Monograph 6, p. 101–111.

Mason, R., and Melnik, N., 1986, The anatomy of an Archean gold system—the McIntyre-Hollinger complex at Timmins, Canada, *in* Macdonald, A.J., ed., Gold '86: Willowdale, Ontario, Konsult International Inc., p. 40–55.

McCuaig, T.C., and Kerrich, R., 1998, P-T-t-deformation-fluid characteristics of lode gold deposits: Evidence from alteration systematics: Ore Geology Reviews, v. 12, p. 381–435.

McCuaig, T.C., Kerrich, R., Groves, D.I., and Archer, N., 1993, The nature and dimensions of regional and local gold-related hydrothermal alteration in tholeiitic metabasalts in the Norseman goldfields: The missing link in a crustal continuum of gold deposits: Mineralium Deposita, v. 28, p. 420–435.

McCuaig, T.C., Behn, M., Stein, H., Hagemann, S.G., McNaughton, N.J., Cassidy, K.F., Champoin, D., and Wyborn, L., 2001, The Boddington gold mine: A new style of Archean Au-Cu deposit [ext. abs.]: AGSO, Geoscience Australia Record 2001/37, p. 453–455.

McKinstry, H.E., 1955, Structure of hydrothermal ore deposits: Economic Geology 50th Anniversary Volume, p. 170–225.

McNaughton, N.J., Mueller, A.G., and Groves, D.I., in press, The age of mineralization in the Golden Mile at Kalgoorlie, Yilgarn craton, Western Australia, determined by SHRIMP U-Pb zircon dating of a synmineralization lamprophyre dike: Economic Geology, v.

Mercier-Langevin, P., Dubé, B., Hannington, M.D., Davis, D., and Lafrance, B., 2004, Contexte géologique et structural des sulfures massifs volcanogènes aurifères du gisement LaRonde, Abitibi. Ministères des Resources naturelles de la faune et des parcs ET 2003–03, 60 p.

Meyer, C., 1981, Ore-forming processes in geologic history: Economic Geology 75th Anniversary Volume, p. 6–41.

MERQ-OGS, 1983, Lithostratographic map of the Abitibi subprovince: Ontario Geological Survey/Ministère de l'Énergie et des Ressources, Québec, 1:500000, catalogued as Map 2428 in Ontario and DV83–16 in Québec.

Mikucki, E.J., and Roberts, F.I., 2004, Metamorphic petrography of the Kalgoorlie region, Eastern Goldfields granite-greenstone terrane: METPET database: Western Australia Geological Survey Record 2003/12, 40 p.

Morasse, S., Wasteneys, H., Cormier, M., Helmstaedt, H., and Mason, R., 1995, A pre-2686 Ma intrusion-related gold deposit at the Kiena mine, Val d'Or, Quebec, southern Abitibi subprovince: Economic Geology, v. 90, p. 1310–1321.

Mueller, A.G., and Groves, D.I., 1991, The classification of Western Australian greenstone-hosted gold deposits according to wallrock-alteration mineral assemblages: Ore Geology Reviews, v. 6, p. 291–331.
Mueller, A.G., Campbell, I.H., Schiotte, L., Sevigny, J.H., and Layer, P.W., 1996, Constraints on the age of granitoid emplacement, metamorphism, gold mineralization, and subsequent cooling of the Archean greenstone terrane at Big Bell, Western Australia: Economic Geology, v. 91, p. 896–915.
Mueller, A.G., Nemchin, A.A., and Frei, R., 2004, The Nevoria gold skarn deposit, Southern Cross greenstone belt, Western Australia: II. Pressure-temperature-time path and relationships to postorogrnic granites: Economic Geology, v. 99, p. 453–478.
Mueller, W., and Donaldson, J.A., 1992, Development of sedimentary basins in the Archean Abitibi belt, Canada: An overview: Canadian Journal of Earth Sciences, v. 29, p. 2249–2265.
Muir, T.L., 2002, The Hemlo gold deposit, Ontario, Canada: Principal deposit characteristics and constraints on mineralization: Ore Geology Reviews, v. 21, p. 1–66.
Myers, J.S., 1995, The generation and assembly of an Archean supercontinent: Evidence from the Yilgarn craton, Western Australia: Geological Society Special Publication 95, p.143–154.
Nelson, D.R., 1997, Evolution of the Archean granite-greenstone terranes of the Eastern Goldfields, Western Australia: SHRIMP U-Pb zircon constraints: Precambrian Research, v. 83, p. 57–81.
Newton, P.G.N., Tornatora, P.M.A., Smith, R., and Clifford, M., 2002, The Cleo-Sunrise deposit, Laverton, WA: Contrasting structural styles within a thrust duplex: Australian Institute of Geoscientists, v. 36, p. 152–155.
Nguyen, T.P., 1997, Structural controls on gold mineralization at the Revenge mine and its tectonic setting in the Lake Lefroy area, Kambalda, Western Australia: Unpublished Ph.D. thesis, Nedlands, University of Western Australia, 195 p.
Ojala, V.J., 1995, Structural and depositional controls on gold mineralisation at the Granny Smith mine, Laverton, Western Australia: Unpublished Ph.D. thesis, Nedlands, University of Western Australia, 184 p.
Ojala, J.V., Ridley, J.R., Groves, D.I., and Hall, G.C., 1993, The Granny Smith gold deposit: The role of heterogeneous stress distribution at an irregular granitoid contact in a greenschist facies terrane: Mineralium Deposita, v. 28, p. 409–419.
Ojala, V.J., McNaughton, N.J., Ridley, J.R., Groves, D.I., and Fanning, C.M., 1997, The Archaean Granny Smith gold deposit, Western Australia: Age and Pb-tracer studies: Chronique de la Recherche Miniere, no. 529, p. 75–89.
Penczak, R.S., and Mason, R., 1997, Metamorphosed Archean epithermal Au-As-Sb-Zn-(Hg) vein mineralization at the Campbell mine, northwestern Ontario: Economic Geology, v. 92, p. 696–719.
——1999, Characteristics and origin of Archean premetamorphic hydrothermal alteration at the Campbell gold mine, northwestern Ontario: Economic Geology, v. 94, p. 507–528.
Percival, J.A., 2003, Superior province: A billion year record of Archean craton evolution and the birth of plate tectonic processes: GAC Howard Street Robinson Distinguished Lecture 2003: Geological Association of Canada Miscellaneous Publication, v. 4, CD ROM.
Perring, C.S., Barley, M.E., Cassidy, K.F., Groves, D.I., McNaughton, N.J., Rock, N.M.S., Betteney, L.F., Golding, S.E., and Hallberg, J.A., 1989, The association of linear orogenic belts, mantle-crustal magmatism, and Archean gold mineralization in the eastern Yilgarn block of Western Australia: Economic Geology Monograph 6, p. 571–584.
Phillips, G.N., 1985, Interpretation of Big Bell/Hemlo-type gold deposits: Precursors, metamorphism, melting and genetic constraints: Transactions of the Geological Society of South Africa, v. 88, p. 159–173.
——1986, Geology and alteration in the Golden Mile, Kalgoorlie: Economic Geology, v. 81, p. 779–808.
Phillips, G.N., Groves, D.I., and Martyn, J.E., 1984, An epigenetic origin for Archean banded iron-formation-hosted gold deposits: Economic Geology, v. 79, p. 162–171.
Pidgeon, R.T., and Hallberg, J.A., 2000, Age relationships in supracrustal sequences of the northern part of the Murchison terrane, Archaean Yilgarn craton, Western Australia: A combined field and zircon U-Pb study: Australian Journal of Earth Sciences, v. 47, p. 153–165.
Powell, W.G., Carmichael, D.M., and Hodgson, C.J., 1995a, Conditions and timing of metamorphism in the southern Abitibi greenstone belt, Quebec: Canadian Journal of Earth Sciences, v. 32, p. 787–805.
Powell, W.G., Hodgson, C.J., Hanes, J.A., Carmichael, D.M., McBride, S., and Farrar, E., 1995b, $^{40}Ar/^{39}Ar$ geochronological evidence for multiple postmetamorphic hydrothermal events focused along faults in the southern Abitibi greenstone belt: Canadian Journal of Earth Sciences, v. 32, p. 768–786.
Price P., and Bray, R.C.E., 1948, Pamour mine, *in* Structural Geology of Canadian Ore Deposits: Montreal, Canadian Institute of Mining and Metallurgy, p. 558–565.
Proudlove, D.C., Hutchinson, R.W., and Rogers, D. S., 1989, Multiphase mineralization in concordant and discordant gold veins, Dome mine, Southe Porcupine, Ontario, Canada: Economic Geology Monograph 6, p. 112–123.
Pyke, D.R., 1982, Geology of the Timmins area: Ontario Geological Survey Geology Report 219, 141 p.
Qiu, Y., and McNaughton, N.J., 1999, Source of Pb in orogenic lode-gold mineralisation: Pb isotopic constraints from deep crustal rocks from the southwestern Archaean Yilgarn craton, Australia: Mineralium Deposita, v. 34, p. 366–381.
Rive, M., Pinson, H., and Ludden, J.N., 1990, Characteristics of late Archean plutonic rocks from the Abitibi and Pontiac subprovinces: Canadian Institute of Mining and Metallurgy Special Volume 43, p. 65–76.
Robert, F., 2001, Syenite-associated disseminated gold deposits in the Abitibi greenstone belt, Canada: Mineralium Deposita, v. 36, p. 503–516.
Robert, F., and Brown, A.C., 1986, Archean gold-quartz veins at the Sigma mine, Abitibi greenstone belt, Quebec. Part I: Geologic relations and formation of the vein system: Economic Geology, v. 81, p. 578–592.
Robert, F., and Poulsen, K.H., 1997, World-class Archaean gold deposits in Canada: An overview: Australian Journal of Earth Sciences, v. 44, p. 329–351.
——2001, Vein formation and deformation in greenstone gold deposits: Reviews in Economic Geology, v. 14, p. 111–155.
Rogers, D.S., 1982, The geology and ore deposits of the No. 8 shaft area, Dome mine: Canadian Institute of Mining and Metallurgy Special Volume 24, p. 161–168.
Ropchan, J.R., Luinstra, B., Fowler, A.D., Benn, K., Ayer, J., Berger, B., Dahn, R., Labine, R., and Hamelin, Y., 2002, Host-rock and structural controls on the nature and timing of gold mineralization at the Holloway mine, Abitibi subprovince, Ontario: Economic Geology, v. 97, p. 291–309.
Ross, A.A., Barley, M.E., Brown, S.J.A., McNaughton, N.J., Ridley, J.R., and Fletcher, I.R., 2004, Young porphyries, old zircons: New constraints on the timing of deformation and gold mineralization in the Eastern Goldfields from SHRIMP U-Pb zircon dating at the Kanowna Belle gold mine, Western Australia: Precambrian Research, v. 128, p. 105–142.
Roth, E., Anderson, G., Daley, L., Groves, D.I., and Staley, R., 1991, Primary mineralization at the Boddington gold mine, western Australia: An Archean porphyry Cu-Au-Mo deposit, *in* Ladeira, E.A., ed., Brazil Gold '91: Rotterdam, A. A. Balkema, p. 418–488.
Rowe, R.J., Awan, A.M., McCuaig, T.C., Sauter, P.C., and Vickery, N.M., 2002, Structural geology of the Plutonic gold mine: Australian Institute of Geoscientists Bulletin 36, p. 180–185.
Salier, B.P., Groves, D.I., Mc Naughton, N.J., and Fletcher, I.R., 2004, The world-class Wallaby gold deposit, Laverton, Western Australia: An orogenic-style overprint on a magmatic-hydrothermal magnetite-calcite alteration pipe?: Mineralium Deposita, v. 39, p. 473–494.
Sanborn-Barrie, M., Skulski, T., and Parker, J., 2001, Three hundred million years of tectonic history recorded by the Red Lake greenstone belt, Ontario: Geological Survey of Canada, Current Research 2001–C19, 30 p.
——2004, Geology, Red Lake greenstone belt, western Superior province: Geological Survey of Canada Open File Report 4594, scale 1:50,000 (with tables and marginal notes).
Scott, C.R., Mueller, W.U., and Pilote, P., 2002, Physical volcanology, stratigraphy, and lithogeochemistry of an Archean volcanic arc: Evolution from plume-related volcanism to arc rifting of SE Abitibi greenstone belt, Val d'Or, Canada: Precambrian Research, v. 115, p. 223–260.
Simmons, S.F., White, N.C., and John, D.A., 2005, Geological characteristics of epithermal precious and base metal deposits: Economic Geology 100TH Anniversary Volume, p. 485–522.
Skulski, T., and Villeneuve, M., 1999, Geochronological compilation of the Superior province, Manitoba, Ontario, Quebec: Geological Survey of Canada Open File Report 3715.
Spooner, E.T.C., 1993, Magmatic sulphide/volatile interaction as a mechanism for producing chalcophile element enriched, Archean Au-quartz, epithermal Au-Ag and Au skarn hydrothermal ore fluids: Ore Geology Reviews, v. 7, p. 359–379.

Stott, G.M., 1997, The Superior province, Canada: Oxford Monograph on Geology and Geophysics, v. 35, p. 480–505.
Stott, G.M., and Corfu, F., 1991, Uchi subprovince: Ontario Geological Survey Special Volume 4, pt. 1, p. 145–236.
Sutcliffe, R.H., Barrie, C.T., Burrows, D.R., and Beakhouse, G.P., 1993, Plutonism in the southern Abitibi subprovince: A tectonic and petrogenetic framework: Economic Geology, v. 88, p. 1359–1375.
Swager, C.P., 1989, Structure of Kalgoorlie greenstones—regional deformation history and implications for the structural setting of the Golden Mile gold deposits: Western Australia Geological Survey Report 25, p. 59–84.
——1997, Tectono-stratigraphy of the late Archaean greenstone terranes in the southern Eastern Goldfields, Western Australia: Precambrian Research, v. 83, p. 11–42.
Thompson, P.E., 2003, Toward a new metamorphic framework for gold exploration in the Red Lake greenstone belt: Ontario Geological Survey Open File Report 6122, 52 p.
Thompson, P.H., 2004, Discover Abitibi. metamorphic subproject. Metamorphic zones and gold exploration targets east of Timmins: Interim report: Ontario Geological Survey Open File Report 6145, p. 45–1 to 45–12.
Thurston, P.C., and Breaks, F.W., 1978, Metamorphic and tectonic evolution of the Uchi-English River subprovince: Geological Survey of Canada Paper 78–10, p. 49–62.
Thurston, P.C., and Chivers, K.M., 1990, Secular variation in greenstone sequence development emphasizing Superior province, Canada: Precambrian Research, v. 46, p. 21–58.
Turek, A., Keller, R., Van Schmus, W.R., and Weber, W., 1989, U-Pb zircon ages for the Rice Lake area, southeastern Manitoba: Canadian Journal Earth Sciences, v. 26, p. 23–30.
Turneaure, F.S., 1955, Metallogenic provinces and epochs: Economic Geology 50th Anniversary Volume, p. 38–98.
Vielreicher, N.M., Groves, D.I., Fletcher, I.R., McNaughton, N.J., and Rasmussen, B., 2003, Hydrothermal monazite and xenotime geochronology: A new direction for precise dating of orogenic gold mineralization: Society of Economic Geologists Newsletter 53, p. 1, 10–15.
Wallace, H., Thurston, P.C., and Corfu, F., 1986, Developments in stratigraphic correlation: Western Uchi subprovince: Ontario Geological Survey MP 129, p. 88–102.
Weinberg, R.F., Moresi, L., and van der Borgh, P., 2003, Timing of deformation in the Norseman-Wiluna belt, Yilgarn craton, Western Australia: Precambrian Research, v. 120, p. 219–239.
Weinberg, R.F., Hodkiewicz, P.F., and Groves, D.I., 2004, What controls gold distribution in Archean terranes?: Geology, v. 32, p. 545–548.
Wilkinson, L., Cruden, A.R., and Krogh, T.E., 1999, Timing and kinematics of post-Timiskaming deformation within the Larder Lake-Cadillac deformation zone, southwest Abitibi greenstone belt, Ontario, Canada: Canadian Journal of Earth Sciences, v. 36, p. 627–647.
Williams, P.R., and Currie, K.L., 1993, Character and regional implications of the sheared Archean granite-greenstone contact near Leonora, Western Australia: Precambrian Research, v. 62, p. 343–367.
Wong, L., Davis, D.W., Krogh, T.E., and Robert, F., 1991, U-Pb zircon and rutile chronology of Archean greenstone formation and gold mineralization in the Val d'Or region, Quebec: Earth and Planetary Science Letters, v. 104, p. 325–336.
Wyman, D.A., Kerrich, R., and Groves, D.I., 1999, Lode gold deposits and Archean mantle plume-island arc interaction, Abitibi subprovince, Canada: Journal of Geology, v. 107, p. 715–725.
Wyman, D.A., Kerrich, R. and Polat, A., 2002, Assembly of Archean cratonic mantle lithosphere and crust: plume-arc interaction in the Abitibi-Wawa subduction-accretion complex: Precambrian Research, v. 115, p. 37–62.
Yeats, C.J., McNaughton, N.J., and Groves, D.I., 1996, SHRIMP U-Pb geochronological constraints on Archean volcanic-hosted massive sulfide and lode gold mineralization at Mount Gibson, Yilgarn craton, Western Australia: Economic Geology, v. 91, p. 1354–1371.
Yeats, C.J., Kohler, E.A., McNaughton, N.J., and Tkatchyk, L.J., 2001, Geological setting and SHRIMP U-Pb geochronological evidence for ca. 2680–2660 Ma lode gold mienralization at Jundee-Nimary in the Yilgarn craton, Western Australia: Mineralium Deposita, v. 36, p. 125–136.
Zweng, P.L., Mortensen, J.K., and Dalrymple, G.B., 1993, Thermochronology of the Camflo gold deposit, Malartic, Quebec: Implications for magmatic underplating and the formation of gold-bearing quartz veins: Economic Geology, v. 88, p. 1700–1721.